

## Polyelectrolyte-induced aggregation of liposomes: a new cluster phase with interesting applications

This article has been downloaded from IOPscience. Please scroll down to see the full text article.

2009 J. Phys.: Condens. Matter 21 203102

(<http://iopscience.iop.org/0953-8984/21/20/203102>)

View [the table of contents for this issue](#), or go to the [journal homepage](#) for more

Download details:

IP Address: 129.252.86.83

The article was downloaded on 29/05/2010 at 19:41

Please note that [terms and conditions apply](#).

## TOPICAL REVIEW

# Polyelectrolyte-induced aggregation of liposomes: a new cluster phase with interesting applications

F Bordi, S Sennato and D Truzzolillo

Dipartimento di Fisica, Università di Roma 'La Sapienza', Piazzale Aldo Moro 5, I-00185 Rome, Italy

and

CRS CNR-INFM 'SOFT', Università di Roma 'La Sapienza', Piazzale Aldo Moro 5, I-00185 Rome, Italy

Received 12 March 2009

Published 24 April 2009

Online at [stacks.iop.org/JPhysCM/21/203102](http://stacks.iop.org/JPhysCM/21/203102)

## Abstract

Different charged colloidal particles have been shown to be able to self-assemble, when mixed in an aqueous solvent with oppositely charged linear polyelectrolytes, forming long-lived finite-size mesoscopic aggregates. On increasing the polyelectrolyte content, with the progressive reduction of the net charge of the primary polyelectrolyte-decorated particles, larger and larger clusters are observed. Close to the isoelectric point, where the charge of the adsorbed polyelectrolytes neutralizes the original charge of the particles' surface, the aggregates reach their maximum size, while beyond this point any further increase of the polyelectrolyte-particle charge ratio causes the formation of aggregates whose size is progressively reduced. This re-entrant condensation behavior is accompanied by a significant overcharging. Overcharging, or charge inversion, occurs when more polyelectrolyte chains adsorb on a particle than are needed to neutralize its original charge so that, eventually, the sign of the net charge of the polymer-decorated particle is inverted. The stability of the finite-size long-lived clusters that this aggregation process yields results from a fine balance between long-range repulsive and short-range attractive interactions, both of electrostatic nature. For the latter, besides the ubiquitous dispersion forces, whose supply becomes relevant only at high ionic strength, the main contribution appears due to the non-uniform correlated distribution of the charge on the surface of the polyelectrolyte-decorated particles ('charge-patch' attraction). The interesting phenomenology shown by these system has a high potential for biotechnological applications, particularly when the primary colloidal particles are bio-compatible lipid vesicles. Possible applications of these systems as multi-compartment vectors for the simultaneous intra-cellular delivery of different pharmacologically active substances will be briefly discussed.

(Some figures in this article are in colour only in the electronic version)

## Contents

1. Introduction	2	3.2. Polyelectrolyte adsorption	8
2. A complex phenomenology	4	4. Electrical transport properties	12
3. Adsorption of polyelectrolytes on the oppositely charged particle surface	7	4.1. The effective charge of colloidal particles	12
3.1. Morphological aspects	8	4.2. Counterion release on polyelectrolyte adsorption	13
		5. Modeling the inter-particle potential	15
		5.1. Monte Carlo simulation and the thermal activated process	17

5.2. A step further	18
6. Possible biomedical applications: developing a new class of vectors for multi-drug delivery	21
6.1. Polyelectrolyte–colloidal particle assemblies as multi-compartment vectors for multi-drug delivery	22
7. Conclusions and perspectives	23
Acknowledgments	24
References	24

## 1. Introduction

Different charged colloidal particles, when mixed in an aqueous solvent with oppositely charged linear polyelectrolytes, have been recently shown to be able to self-assemble, forming long-lived, finite-size mesoscopic aggregates [1, 2].

Due to the rapid adsorption of the polyelectrolytes on the oppositely charged particles, the contribution of osmotic forces originating from depletion effects, which are usually the dominating interaction that drive the particles' aggregation when non-adsorbing polymers are added to a colloidal suspension, is negligible. The search for an explanation of the complex phenomenology observed in these systems must hence proceed in a different direction.

There is accumulating evidence that in these systems, once the polyelectrolytes are adsorbed at the particle surface, and the adsorption, due to the repulsion between the like-charged chains, occurs in a correlated manner, the *polyelectrolyte-decorated particles* (pd particles hereafter) interact through a complex inter-particle potential which is mainly of electrostatic nature. As we will see, this interaction results from the superposition of screened electrostatic repulsions, due to the residual net charge of the pd particles, and attractive electrostatic forces, due to the non-uniform distribution of the surface charge, with an important short-ranged contribution of dispersion forces. For the resulting adhesive effect of the adsorbed polyelectrolytes there has been coined the suggestive name of 'electrostatic glue' [3]. However, despite the increasing body of experimental and theoretical work [1–12], what the detailed mechanism is that in these systems drives the aggregation and stabilizes a well-defined size of the clusters, which changes with the polymer/particle ratio, is still a much debated question.

One of the mechanisms that in a colloidal suspension drives the formation of clusters of the primary particles is phase separation, where the system lowers its free energy by splitting into a colloid-poor 'gas' and a colloid-rich 'liquid' [13]. Alternatively, clusters could simply assemble by adding more and more primary particles, which stick irreversibly upon approaching in a diffusion-controlled kinetic process [14]. In both cases, the aggregates are not expected to reach a maximum size and, after that, to remain stable in time. In fact, in one case, the growth of the colloid-rich droplets, being thermodynamically favored, would proceed until either all of them coalesce together and the system results ultimately separated into two phases or, being the phase separation frustrated by a kinetic arrest, the system forms a gel [15]. In the other case, within the framework of the classical

diffusion-limited cluster aggregation (DLCA) [14], clusters keep growing until, in principle, all the primary particles are gathered together in one single aggregate (corresponding to a phase separation). In practice, when the aggregates become very large, their further growth is prevented by the progressive reduction of their mobility, which makes the probability of an encounter negligible.

The formation of stable diffusing clusters in colloids has been justified in terms of a competition between short-range attraction and long-range electrostatic repulsion [16–19]. Within this scheme, after clusters had grown to a certain size, they would have accumulated enough charge to repel additional particles. The new length scale introduced by such 'intra-cluster', long-range Coulombic repulsion characterizes the maximum size [13, 16–18, 20] reached by the aggregates. Clearly, for this mechanism to be effective in producing large clusters, the range of electrostatic repulsions should be of the same order as the primary particle size at least, or larger. In a solution, the effective range of Coulombic interactions is usually expressed as the Debye screening length  $\kappa^{-1} = [4\pi l_B \sum_i C_i Z_i^2]^{1/2}$ , in terms of the number concentrations,  $C_i$ , of the ions of valence,  $Z_i$ , and of the Bjerrum length  $l_B = \frac{e^2}{4\pi\epsilon_0\epsilon_r K_B T}$  (on this length, the energy of the electrostatic interaction between two elementary charges  $e$  immersed in a medium with relative dielectric permittivity  $\epsilon_r$  is equal to the thermal energy  $K_B T$ ).

In fact, stable colloidal cluster phases are observed in several different systems where low charged primary particles are dispersed in a low permittivity medium [16, 17, 20]. In these conditions the effective range of the Coulombic repulsions can be easily made several times the typical diameter of the primary particles. Conversely, in aqueous solutions of highly charged colloidal particles, and even more in the presence of highly charged linear polyelectrolytes, due to the high permittivity and to the relatively high ionic strength of the solution, the screening length is typically of the order of ten nanometers or less, i.e. much shorter than the typical size of colloidal particles. As an example, at  $T = 25^\circ\text{C}$  in water and in the presence of a molar concentration of monovalent ions of  $10^{-2}\kappa^{-1}$  it is  $\approx 10$  nm. These considerations suggest that the formation of the observed long-lived particle clusters in a polyelectrolyte–colloid system cannot be justified simply on the basis of the equilibrium between short-range attractions and a long-range electrostatic repulsion.

Finally, the intuitive explanation of the observed aggregation based on a simple 'bridging' mechanism, with the colloidal particles joined like beads of a necklace by polyelectrolyte chains that partially adsorb on different particles, is to be ruled out, since relatively short polyelectrolytes compared to the size of the particles are also sufficient to induce the aggregation [6]. Moreover, due to the high charge densities that characterize the particles and the polyelectrolytes in these systems, the chains tend to remain rather flat when adsorbed on the particle surface [21–23]. Besides, the formation of the aggregates is observed also at very low volume fractions (of the order of 0.1%). In this condition, owing to the strong attraction of the chain to the surface and to the large difference in the timescales of adsorption and diffusion, the probability that two

sections of a relatively short chain adsorb simultaneously on two different particles is very low. Finally, the bridging mechanism would not justify the finite size of the aggregates also for the shorter chains, nor the re-entrant dependence of this size on the polymer–particle charge ratio.

The formation of the long-lived, finite-size, diffusing clusters observed in pd colloids in aqueous solution must hence be the result of a somewhat different and more subtle mechanism.

Although, in principle, even in the case of a uniform coverage of the particles with a soft, penetrable layer, or brush, of like-charged polymers on their surface, an attractive inter-particle force can be generated [24], a key role is apparently played by the correlation between the adsorbed polyelectrolyte chains on the surface of the oppositely charged particles. In fact, due to the competing interactions between the polyelectrolyte and the surface (attractive) and between the like-charged polymers (repulsive), the adsorbed chains are locally ordered: the polyelectrolyte chains adsorb in a *correlated* way [25–31]. It is to stress this aspect of the correlation that we rather talk in terms of polyelectrolyte *decorated* particles instead of, for example, *coated* particles.

The correlated adsorption results in a non-uniform distribution of the electric charge at the particle surface, which shows domains or patches with alternating signs, where the polymer charge is locally in excess or the charge of the bare particle surface prevails. As Velegol and Twar [32] have recently shown, a non-uniform distribution of the electric charge on the surface of colloidal particles results in an inter-particle potential that, even in the case of like-charged particles, has an attractive component. This potential depends on the values of the electrostatic surface potential,  $\Phi$ , averaged on the whole particle surface and on its standard deviation  $\sigma$ . For some combinations of  $\Phi$  and  $\sigma$  this inter-particle potential shows a maximum close to the particles' surface. This is the energy barrier that two approaching particles must overcome before sticking together. Interestingly, the height of this barrier increases with the radius of curvature,  $R$ , of the particles.

To a first approximation, a 'drop-like' growth can be assumed for large enough clusters, i.e. an effective radius of curvature of the aggregate surface which increases with the aggregation number. This assumption is consistent with the experiments in the case of deformable primary particles such as, for example, polyelectrolyte-decorated lipid vesicles [11], and appear reasonable for large enough and sufficiently compact aggregates. With this assumption, the presence of a size-dependent potential barrier could justify the formation of metastable finite-size clusters. In fact, for large enough aggregates, the proportion of collisions sufficiently energetic to overcome the barrier becomes negligible. The same effect also opposes the development of sharp protrusions that, representing local 'seeds' for the adhesion of further (deformable) particles, tend to be leveled, favoring the growth of the aggregates as rather compact objects.

On the other hand, the *correlated* adsorption of the polyelectrolyte chains is also the cause of the counterintuitive phenomenon of the 'overcharging', or charge inversion [28–31], a

well-known phenomenon in the case of the adsorption of multi-valent ions on an oppositely charged surface, which is also observed for pd particles. This phenomenon occurs when more polyelectrolyte adsorbs on a particle than is needed to neutralize its original charge so that, eventually, the net charge of the polymer-decorated particle inverts its sign.

The attractive component of the inter-particle potential, and the progressive variation of the net charge of the decorated particles, down to the neutralization point and up again to the maximum overcharging, both consequences of the *correlated* adsorption of the polyelectrolyte, combine together to give rise to a peculiar phenomenon of 're-entrant condensation' of the pd particles.

As the polyelectrolyte/particle ratio is increased, associated with the progressive reduction of the net charge of the primary polyelectrolyte-decorated particles, larger and larger clusters are observed. Close to the isoelectric condition the aggregates reach their maximum size, while beyond this point any further increase of the polyelectrolyte–particle charge ratio causes the formation of aggregates whose size is progressively reduced ('re-entrant condensation'). Eventually, when the surface of the particles is completely saturated by the adsorbed polyelectrolyte, i.e. the overcharging has reached its maximum extent, the size of the particles in the suspension equals again the size of the original colloidal particles, plus a thin layer of adsorbed polymer [2, 6, 8]. From here on, by further increasing the polymer/particle ratio, the excess polyelectrolyte, that does not adsorb any more on the particles, remains 'freely' dissolved, contributing to the overall ionic strength of the solution. Finally, when the ionic strength grows beyond a given threshold, and any residual Coulomb repulsion is screened, the colloid is completely destabilized and every collision results in adhesion. Then, independently of how this condition has been obtained, whether by increasing the polyelectrolyte concentration or by adding some simple salt to the solution, the particles invariably coagulate [33]. It is worth stressing that this coagulation, which occurs at much higher polyelectrolyte/particle ratios than the 're-entrant condensation', is an irreversible phenomenon that ultimately results in the complete separation of the solid phase (flocculation) and that can be well described within the framework of the classical DLVO theory [14].

This complex phenomenology has been observed in a variety of polyelectrolyte–colloid systems dispersed in aqueous solutions such as, for example, polyelectrolyte–micelle complexes [5], latex particles [12, 34], dendrimers [35], ferric oxide particles [36], phospholipid vesicles (liposomes) [1, 2, 37] and 'hybrid niosome' vesicles [38]. Although the adsorption can be further complicated by the presence of short-range interactions, specific to the different components, the similarities in the observed behavior for such different systems strongly indicate that the overall phenomenology is mainly governed by non-specific electrostatic interactions, arising from double-layer overlap (repulsion) and surface charge non-uniformity (attraction).

This review is organized as follows. In section 2 the dynamics of the aggregation and the morphology of the resulting aggregates will be briefly discussed. The case of pd-liposome aggregates will be considered in detail, due

to the high potential for biotechnological applications of this system. The ‘multi-compartment’ structure of these aggregates, where the single lipid vesicles maintain their individuality and their separate contents, will be described and some experimental evidence of this structure will be discussed. In section 3 the recent literature on the adsorption of polyelectrolytes at the oppositely charged surface of the colloidal particles, and on the overcharging phenomenon, will be briefly reviewed. The interesting and still controversial issue of the extent of the release of condensed counterions from the adsorbing polyelectrolytes, and the role that this release would play in favoring the aggregation of the polyelectrolyte-decorated liposomes, will be briefly discussed in section 4. Section 5 is devoted to a discussion of a possible model for the inter-particle interaction. Simulations based on this model seem to be able to reproduce the different aspects of the complex phenomenology observed. Finally, in section 6 possible biotechnological applications of the multi-compartment aggregates resulting from the polyelectrolyte-induced aggregation of colloidal particles will be briefly discussed.

## 2. A complex phenomenology

As an example of the ‘re-entrant condensation’ that is observed when a polyelectrolyte is added to a suspension of oppositely charged colloidal particles, figure 1 shows the evolution of the hydrodynamic radius  $R$  for the complexes of cationic lipid vesicles with a synthetic polyelectrolyte as a function of the stoichiometric polyelectrolyte/lipid charge ratio  $\xi = C_p/C_L$ .  $C_p$  and  $C_L$  are the equivalent concentrations (mole of charge per liter) of the polyelectrolyte and of the lipid, respectively. In other words,  $\xi$  (hereafter, the charge ratio) can also be defined as the ratio  $\xi = N_p/N_L$  of the stoichiometric charge of the polymer ( $N_p$ ) to the total number of the charged groups on the lipids ( $N_L$ ). In this example (data from [39]) the colloidal particles are uni-lamellar liposomes, with an average diameter of  $\approx 80$  nm, built up with a synthetic lipid, DOTAP (1,2-dioleoyl-3-trimethyl ammonium propane). Their aggregation is induced by adding to the suspension increasing amounts of an anionic synthetic polyelectrolyte, sodium polyacrylate (NaPA). For each measurement an independent sample is employed, prepared by mixing in one single step proper amounts of the aqueous solutions of the polyelectrolyte and of the liposomes, and gently handshaking.

At low polyelectrolyte content, the hydrodynamic diameter  $\langle 2R \rangle$  of the complexes, measured by dynamic light scattering (intensity-averaged size distribution [40]), is, within the experimental uncertainties, equal to the size of the original liposomes. With the increase of the polyelectrolyte content, the size of the complexes increases up to a maximum of the order of a few micrometers, which is attained at  $\xi \approx 1$ , close to the neutralization point, where the  $\zeta$  potential measured for the aggregates is zero. Beyond this point, the size of the aggregates decreases again to a final value slightly larger than that measured for the native vesicles, consistent with liposomes coated by a polyelectrolyte layer [6]. It must be noted that very close to the isoelectric point they form huge aggregates. Within

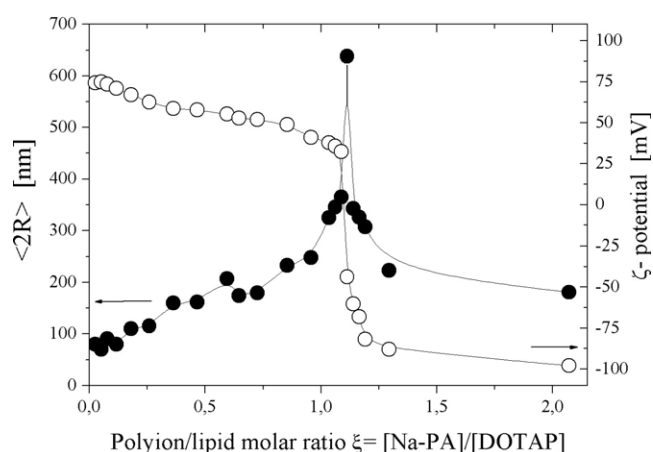


**Figure 1.** Average hydrodynamic diameter  $\langle 2R \rangle$  (●) and  $\zeta$  potential (○) of NaPA–DOTAP complexes as a function of the polyion/DOTAP molar charge ratio parameter  $\xi$ . Data adapted from [39].

the narrow range of polyelectrolyte concentrations where this maximum of the aggregation is observed, it is difficult to determine experimentally the exact size of the aggregates and especially their zeta potential. However, the observed dielectric behavior of the suspensions close to the isoelectric point is consistent with a zeta potential of the aggregates that goes to zero smoothly in correspondence to the peak in the particles’ size distribution [41].

A qualitatively analogous behavior has been observed also for polyelectrolyte–liposome systems where the vesicles have a different surface charge density [42], or where the charge of the two components is inverted (anionic vesicles and cationic polyelectrolytes) [2, 38]. Also the specific structure of the polyelectrolyte employed does not affect significantly the overall characteristics of the re-entrant condensation behavior that has been observed for complexes of different lipid vesicles with synthetic polyelectrolytes [6, 8, 38, 43], highly charged linear poly-aminoacids [2, 38], polysaccharides [44], and DNA, double [37, 45] or single stranded [45, 46]. This phenomenology does not appear to be restricted to lipid vesicles, since it has been observed also for other charged colloids dispersed in aqueous solutions, such as micelles [5], latex particles [12, 34], ferric oxide particles [36], lipid-coated latex particles [47] and dendrimers [35] in the presence of different oppositely charged linear polyelectrolytes.

Systems where the colloidal particles forming the clusters are lipid vesicles appear particularly interesting due to their potential for biotechnological applications, as we will discuss in section 6. As we will see, due to their affinity for biological cell membranes, lipid vesicles are already widely employed as ‘vectors’ to facilitate the transport of different pharmaceutically active molecules through the cell membrane. The possibility of easily assembling several different vesicles in a single cluster opens the interesting perspective of employing ‘multi-compartment’ (and hence multi-purpose) vectors for the simultaneous and independent delivery of different active substances to the same cell.

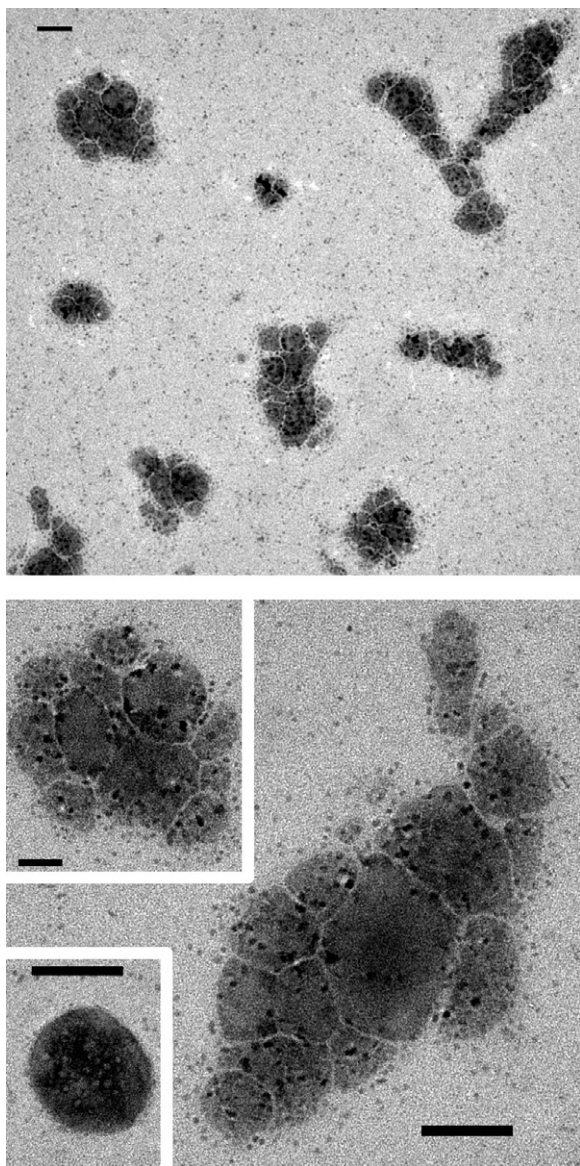


**Figure 2.** Transmission electron microscopy images of typical pd-liposome aggregates. When they are isolated the pd liposomes (lower left small inset) have an approximately spherical appearance. Conversely, within the aggregates, due to the adhesion forces between the adjacent lipid membranes, the contours of the packed vesicles appear flattened. However, the whole aggregates grow, maintaining a compact shape. The bar represents 100 nm. The samples shown are not stained; the observed contrast is obtained by preparing the liposomes with a proper concentration of CsCl in the aqueous core, with a procedure which is described in detail in [1].

For this reason we will consider here in more detail the morphology of the clusters formed by these particular colloids. Figure 2 shows an example of the appearance of the clusters that form when a polyelectrolyte (sodium poly-acrylate in this case) is added to a suspension of oppositely charged lipid vesicles (DOTAP uni-lamellar liposomes).

The small inset shows an isolated liposome (this image has been obtained at very low polyelectrolyte content) with the typical, almost spherical appearance. Conversely, within the aggregates the adjacent lipid membranes, due to a balance

between the adhesion forces and the intrinsic elasticity of the bilayers [48], are flattened. The transmission electron microscope (TEM) images shown in figure 2 were obtained without any staining procedure of the samples. The contrast is obtained by preparing the liposomes with a heavy element (a cesium salt) dissolved in the aqueous core (the procedure is described in detail in [1]). Since the heavy element salt is excluded from the hydrophobic interior of the double layer, in the bi-dimensional TEM images the membranes separating the liposomes within the clusters appear as pale gray lines. In the figure the contours of the vesicles packed into the aggregates appear as (almost) straight segments (suggesting the flattening of the membranes at the contact zones). However, the whole aggregates grow, maintaining a compact appearance, being delimited by a rather smooth surface whose curvature radius increases with the aggregation number. The neat contrast between the interior of the liposomes and the surrounding medium is an indication that the vesicles maintain their inner core separated from the outer medium during the whole aggregation process and that they do not undergo any evident restructuring process, as previously postulated [37, 49–51]. Restructuring processes indeed occur in some systems, but they are apparently connected with the particular structure of the polyelectrolyte, composition of the liposomes and concentration regimes in a complicated and not yet completely understood manner. In the different conditions these systems show a rich scenario of nanostructures and morphologies, from uni-lamellar polyelectrolyte-coated liposomes to multi-lamellar structures, with the polyelectrolyte ‘sandwiched’ between lipid bilayers, passing through cluster-like structures and different intermediate morphologies [50, 52].

In view of the applications of lipid vesicle clusters as ‘multi-compartment’ vectors, the question if the different vesicles maintain in the aggregate their structural integrity and their separate contents is an important issue.

In another experiment [1] a cluster phase was built up where different vesicles within the same aggregate were filled with two different concentration of Cs. These complex structures were obtained simply by mixing two different liposome suspensions prepared at two Cs concentrations and then inducing the aggregation by adding the proper amount of polyelectrolyte. This procedure is an example of how, by exploiting the self-assembling property of these systems, it is possible to build up ‘multi-compartment’ nanostructures in a simple and effective way; nanostructures that, in principle, can be employed for the simultaneous transport of different substances through the biological cell membranes.

That pd-lipid vesicles can maintain their core content unaltered during the aggregation process has also been shown by using electrical conductivity measurements [53]. In this experiment DOTAP liposomes were prepared in a 0.3 M NaCl electrolyte solution. Then, by extensive dialysis against deionized water, the salt was removed from the dispersing medium, reducing the conductivity of the suspension from its initial value. In contrast, the electrolyte within the vesicle core maintained its concentration since it is known that an osmotic difference of this order of magnitude does not produce the rupture of the membrane of small uni-lamellar liposomes [54], which are rather inert to osmotic shock.

However, by sonicating the dialyzed suspension, the electrical conductivity increased again, indicating that this treatment causes the release of the ionic content of the vesicles. By combining light scattering and dielectric measurements it was inferred that sonication did not alter the size nor the volume fraction of the vesicles in the suspension. These findings suggest that the ultrasound treatment simply opens transient pores in the membrane bilayer, allowing the readjusting of the salt concentration between the two sides of the membrane. In fact, the small increase observed in the measured electrical conductivity was in quantitative agreement with what could be calculated on the basis of the volume fraction of the vesicles and of the concentration of the electrolyte in their core [53].

In general, the structure of the bilayer can be perturbed by the adsorbed polyelectrolyte. For example, the polyelectrolyte adsorbed on the outer leaflet of the bilayer can induce the 'flip-flop' (translocation) of oppositely charged lipids from the inner to the outer leaflet. Yaroslavov *et al* [7] have given evidence of this effect in a system where the highly charged polycation poly-vinylpyridine was added to uni-lamellar liposomes composed of egg lecithin or di-palmitoyl-phosphatidyl-choline (DPPC) and cardiolipin (a phospholipid with two negative charges). It is noteworthy that these authors also showed that the zwitterionic polymers prepared by quaternizing poly-vinylpyridine with different bromo-acids induce no flip-flop of cardiolipin, suggesting that the linear charge density of the polyelectrolyte is an important parameter in determining this effect.

The effect of the polyelectrolyte on the membrane ordering can be considerable if its chemical structure favors non-electrostatic interactions with the hydrophobic interior of the bilayer [43, 55–57]. For example, poly-lysine, a highly charged cationic polyelectrolyte, has long been known to be able to induce the fusion and restructuring of lipid membranes with different compositions, or even to migrate through a lipid bilayer [58, 59]. Hybrid niosomes, small uni-lamellar vesicles built up with a mixture of non-ionic (Tween-20) and ionic (dicetylphosphate) surfactants and cholesterol, maintain their content when their aggregation is induced by poly-ethyl-vinyl-pyridinium bromide, PEVP, or  $\epsilon$ -polylysine but show evidence of significant leakage when the adsorbed polyelectrolyte is  $\alpha$ -polylysine [38]. Moreover, while PEVP-hybrid niosome clusters appear stable with time,  $\alpha$ -polylysine aggregates show a marked size instability in a wide region around the isoelectric point. In this region the aggregate size increases with time, with a rate that depends on the polyelectrolyte-lipid charge ratio. Within the same range, fluorescence measurements show evidence of an exchange of matter between the inner core of the vesicles and the surrounding medium, probably due to a structural rearrangement of the membranes within the aggregates or, at least, to a partial rupture of the bilayer continuity.

A similar behavior, with the formation of large unstable aggregates, was observed in other systems built up by  $\alpha$ -polylysine and different negatively charged liposomes [58–62].

The adsorption of  $\alpha$ -polylysine has been shown long ago to be associated with leakages of the content of lipid

vesicles [61]. Hammes *et al* [60], by means of electron microscopy techniques, observed a dramatic rearrangement of the vesicles into large multi-lamellar aggregates when  $\alpha$ -polylysine was added to a suspension of phosphatidyl-serine (PS, an anionic lipid) liposomes. According to Walter *et al* [62], in suspensions of liposomes with mixed bilayers composed of PS and phosphatidyl-choline (PC) (zwitterionic), the  $\alpha$ -polylysine induces the formation of large aggregates and a notable leakage of the liposome content, which are accompanied by the fusion of the vesicles. The extent of these effects depends on the surface charge density of the vesicles, the relative amount of the polyelectrolyte and the pH of the solution. These effects have been generally attributed to the insertion of this particular polyelectrolyte into the double layer, favored by hydrophobic interactions with the aliphatic core of the bilayer. Recently Yaroslavov *et al* [58] even observed the passage of  $\alpha$ -polylysine molecules through the double layer of anionic liposomes. These authors found that  $\alpha$ -polylysine, after forming complexes with the anionic lipids present in the vesicle wall, is then able to pass through the lipid bilayer. In another paper [59] they showed that, when  $\alpha$ -polylysine adsorbs to liposomes made up with cardiolipin (CL, a negatively charged natural lipid) and different lecithins, the permeability of the bilayer to various molecules is enhanced. In particular they measured the rate constant for the bilayer permeation of doxorubicin, a fluorescent anti-tumor drug, showing that in the presence of  $\alpha$ -polylysine its value is almost doubled. Considering that at the pH of the experiments doxorubicin is partially ionized (cationic), this ability of  $\alpha$ -polylysine of facilitating its passage through the bilayer is particularly intriguing. A suggestive hypothesis of the authors to justify this capacity of  $\alpha$ -polylysine of favoring the trans-bilayer transport of like-charged molecules is based on their observation that the binding of  $\alpha$ -polylysine to the membrane surface causes the formation of domains (or 'rafts') of the negatively charged CL in the outer leaflet, that would hence be neutralized by the bound polyelectrolyte chains. The patches, or domains, that resulted from such lateral lipid segregation in the membrane, and/or the boundaries between the patches and the surrounding lipid bilayer, would be responsible for the acceleration of transmembrane doxorubicin permeation [63].

The ability of  $\alpha$ -polylysine to pass through the hydrophobic core of a lipid bilayer suggests a role for non-electrostatic interactions [58, 64]. Raman studies [65] and circular dichroism data [60] give evidence that upon adsorption on negatively charged surfaces  $\alpha$ -polylysine undergoes a conformational change, from random coil to  $\alpha$ -helix. The helix-coil transition is probably an effect of the partial neutralization of the adsorbed poly-lysine due to the presence of the negative charges at the vesicle surface, the reduction of electrostatic repulsions between the different monomers along the chain favoring the  $\alpha$ -helix conformation [66]. On the other hand, it has also been shown that the  $\alpha$ -helix conformers of  $\alpha$ -polylysine are more lipophilic than the random coil conformer [67]. Putting together these two observations, it appears reasonable that the process that, in the presence of  $\alpha$ -polylysine, results in an enhanced permeability of the lipid bilayers and in their tendency to fuse and restructure, probably

occurs in a sequence not much dissimilar from this one: upon adsorption on the surface of the anionic liposomes  $\alpha$ -polylysine, being partially neutralized, undergoes a helix–coil transition; the  $\alpha$ -helix conformers penetrate the double layer, due to their favorable interaction with its hydrophobic interior; the impaired ordering of the bilayer increases its permeability, and it is likely to favor the fusion of adjacent membranes.

Although several aspects of this qualitative picture still need to be clarified, in fact, when  $\alpha$ -polylysine is replaced by  $\varepsilon$ -polylysine, a lysine homopolymer that cannot form  $\alpha$ -helix, niosomal vesicles, which in the presence of  $\alpha$ -polylysine show evident leakages, aggregate according to the re-entrant condensation behavior and form stable clusters, where the integrity of the individual vesicles is preserved and there is no evidence of fusion or leakage [38].

The destabilizing effect of  $\alpha$ -polylysine depends on the concentration regime and on the liposome composition, as demonstrated by the seemingly contradictory results reported in the literature. For example, in a recent paper Volodkin *et al* [2], on the basis of their differential scanning calorimetry measurements, report that the adsorption of  $\alpha$ -polylysine occurs exclusively on the surface of their vesicle (built up with a mixture of DPPC, cholesterol and di-palmitoyl-phosphoglycerol Na salt (DPPG)) and that the lipidic organization is not significantly disturbed by the adsorbed polyelectrolyte. Also the multi-lamellar and/or hexagonal phases that are usually observed when DNA interacts with different cationic liposomes [51, 52, 68, 69] are probably the result of the still not completely understood processes of destabilization and restructuring of the lipid phase induced by the high charge density of this polyelectrolyte. It is probable that also in this case, as in the case of the poly-lysine, there is some contribution of non-electrostatic interactions, and also in this case the destabilizing effect probably depends on the concentration regime. This could explain the seeming contradiction of SAXS experiments (that require rather high volume fractions) where the DNA-induced restructuring of the bilayers is invariably observed [51] and low volume fraction experiments where the vesicles maintain their shape and content [1, 38, 53].

### 3. Adsorption of polyelectrolytes on the oppositely charged particle surface

As we have discussed above, the complex phenomenology of re-entrant condensation and charge inversion has been described for a variety of charged colloids in the presence of different oppositely charged linear polyelectrolytes. In some cases the colloidal particles were solid (bare [12, 34] or lipid-coated [47] latex particles or ferric oxide particles [36]), while in other cases the particles were ‘soft’ lipid vesicles. While in the case of solid latex particles it is obvious that the polyelectrolyte cannot penetrate the particles or cause their ‘restructuring’, and it is simply expected to adsorb on their surface, in the case of lipid vesicles, as we have discussed in detail in the preceding paragraph, there is evidence that, depending on the chemical structure of the polyelectrolyte employed, and due to the possible occurrence

of non-electrostatic interactions with the hydrophobic core, the polymer can penetrate the double layer, causing its destabilization.

In the earlier literature on the complexation of polyelectrolytes with charged lipid vesicles, these two aspects, the formation of long-lived clusters of vesicles ‘glued together’ by the adsorbed polyelectrolyte chains and the restructuring of the bilayers within the aggregates, have not been sufficiently distinguished and the observed re-entrant condensation has often been interpreted, tentatively, as a by-product of the restructuring process. However, there is now accumulating evidence that the concomitant phenomena of the overcharging and of the formation of long-lived, finite-size clusters with a size depending on the polyelectrolyte–particle ratio (re-entrant condensation) are very general, occurring for solid particles as well as for vesicles. Hence they cannot be a consequence of a particular interaction between polyelectrolytes and lipid membranes, and of a ‘restructuring process’ of the lipid bilayers, but must be related to the adsorption of the polyelectrolyte chains at the oppositely charged particle surface.

From this point of view, different models that analyzed the complex electrostatic interaction of lipid bilayers with highly charged linear polyelectrolytes, particularly DNA (for example [49, 70, 71]) in terms of the restructuring process that the charged lipid bilayers undergo in the presence of those macromolecules, although extremely useful to rationalize that peculiar process, do not appear sufficient to describe the initial aggregation that precedes the bilayer reorganization and is a much more general phenomenon in polyelectrolyte oppositely charged colloid systems.

As we will discuss in detail in section 5, a good hypothesis to justify the re-entrant condensation observed in these systems is the existence of an attractive contribution in the inter-particle potential due to the non-uniform distribution of the electric charge on the surface of the polyelectrolyte-decorated particles, a consequence of the correlated adsorption of the polymer chains.

In fact, when a polyelectrolyte solution and a suspension of oppositely charged colloidal particles are mixed together, the adsorption of the polyelectrolyte on the particle surface is a much faster process than the aggregation. The huge surface/volume ratio which characterizes the colloid, and the distribution of this surface within the whole volume of the host phase, speed dramatically the adsorption process, decreasing the time for the polyelectrolyte chains to reach the adsorbing surface by diffusion. Conversely, the aggregation, being controlled by the diffusivity of the bulkier colloidal particles, occurs on longer timescales. This conjecture, which appears reasonable, has been recently substantiated with experimental evidence by Volodkin *et al* [2]. By using different mixing protocols, varying the agitation speed and the order of mixing (e.g. by adding the polyelectrolyte solution to the particle suspension or vice versa), these authors showed that the polyelectrolyte adsorption is almost immediate in comparison with the characteristic times of the aggregation processes that are typical of particle diffusion.

As a consequence of the different timescales, the ‘primary particles’ that are involved in the aggregation process are the polyelectrolyte-decorated particles (pd particles).



This observation suggests a useful shift of the perspective to guide the investigation of this complex phenomenology. Rather than hypothesizing complex scenarios of ‘polyelectrolyte-mediated’ interactions, where the polyelectrolytes drive the aggregation of the colloid by a mix of osmotic, electrostatic screening and bridging effects, one has to deal with a much simpler (but unfortunately still rather complicated) system of non-uniformly charged polymer-decorated particles.

With this in mind, it is then clear the importance of having a detailed understanding of how the adsorption of the chain occurs. A vast literature exists concerning the general issue of the adsorption of polyelectrolyte chains on oppositely charged surfaces, which has been recently and excellently reviewed [28, 72, 73]. For this reason in the following paragraph, we will focus our brief discussion on those aspects that are more relevant to the re-entrant condensation.

### 3.1. Morphological aspects

The main point that deserves to be stressed in the context of the re-entrant aggregation is that the adsorption of the linear polyelectrolytes on the surface of the oppositely charged particles occurs in a highly correlated manner [27–31]. It is to stress this correlation that we rather talk of polyelectrolyte-‘decorated’ particles instead of, for example, ‘coated’ particles.

In fact, the competing interactions between the polyelectrolytes and the surface (attraction) and between the like-charged chains (repulsion) result in a locally ordered, correlated adsorption of the polymer. A non-uniform distribution of the adsorbed chains means a non-uniform distribution of the surface electric charge, showing alternate patches where the charge of the polymer or the particle is locally in excess. As we will see in more detail in section 5, it is from this charge non-uniformity that there arises the attractive component of the inter-particle potential that, together with the screened Coulomb repulsion, concurs in the formation of the finite-size cluster phase observed in these systems.

Direct experimental evidence of the correlation of the polyelectrolyte chains adsorbed on the surface of the colloidal particles within the typical complexes of the re-entrant condensation is furnished by the TEM images of cationic liposome (DOTAP) aggregates induced by different anionic polyelectrolytes [6, 45]. In these images, within the clusters, globular regions with the typical size of the original liposomes ( $\approx 100$  nm) are clearly distinguishable, clearly showing that clusters are composed of liposomes ‘glued together’. However, these globular regions are covered by a characteristic ‘fingerprint’ pattern, which is not visible in the absence of the polyelectrolyte and that has been interpreted as due to the organization of the polyelectrolyte molecules adsorbed at the liposome surface. When double helix DNA was employed as the polyelectrolyte, a two-dimensional Fourier transform analysis of the image gave a characteristic repetition length (the average distance between the centers of two adjacent lines of the ‘fingerprint’ pattern) of  $\approx 4$  nm [45]. This value is in good agreement with the average distance between a DNA helix deposited on planar bilayers of

cationic lipids measured in AFM images by different authors ( $\approx 5$  nm [25] or 6.5 nm [74] for DNA on dipalmitoyl-trimethyl-ammonium-propane (DPTAP) and values between 4.3 and 5.8 nm [75] for DNA on dipalmitoyl-dimethyl-ammonium-propane (DPDAP) or distearoyl-dimethyl-ammonium-propane (DSDAP) at different bulk NaCl concentrations), AFM images that show a ‘fingerprint’ pattern very similar to the one characterizing the surface of liposome–DNA aggregates.

Although the plain correspondence in the appearance of the two systems, in TEM and AFM images, strongly suggests the identical nature of the observed features, similar patterns in TEM images have also been variously interpreted, in the case of DNA–liposome complexes, as a side view of multilayered structures [76, 77]. However, the use of biotinylated DNA to promote the aggregation of cationic liposomes allowed us to show that the DNA is distributed on the whole surface of the aggregates and that the fingerprint pattern is undoubtedly associated with the adsorbed DNA [45]. In that experiment, to create the liposome aggregates biotin-labeled DNA fragments were employed, obtained by polymerase chain reaction (PCR) in the presence of a biotin-conjugated base (biotin-14-dCTP). Streptavidin is a molecule that has a high specific affinity with biotin, so that the biotin-labeled DNA can be easily localized in TEM images by using streptavidin-conjugated gold nanoparticles that selectively bind the biotinylated DNA.

### 3.2. Polyelectrolyte adsorption

The adsorption of polyelectrolytes at charged surfaces from an aqueous solution has been attracting considerable interest for more than two decades [72, 73, 78–80], because of the great importance of this issue in a wide range of technological applications, as well as for its relevance in the understanding of fundamental biological processes. Polyelectrolytes are macromolecules bearing a large number of ionizable groups along their backbone. When dissolved in a polar solvent such as, for example, water, these groups dissociate and the counterions, diffusing into the bulk solution, leave behind an opposite charge [72] on the backbone (polyion). Owing to the fine interplay between the electrostatic attraction of the counterions to the densely charged chains, and the loss of translational entropy that they would suffer, were their motion restricted in the vicinity of the chain by that attraction, these solutions display peculiar behaviors, differing from both neutral polymer solutions and from simple electrolytes.

Polyelectrolytes spontaneously adsorb from solution onto an oppositely charged surface replacing counterions. The adsorbed layers can be thin [21], with the chains lying flat on the surface, or can be more fluffy, with the chains forming loops and dangling ends between ‘adsorption trains’ at the surface in a ‘pseudo-brush’ configuration [81]. Depending on the stiffness of the polyelectrolyte and on charge densities of the chain and the surface, the layer can be flat and compressed or coiled and extended. Which conformation is favored depends mostly on the linear charge density of the polymer and the charge density of the surface; more, in general, on a balance between the strength of the (electrostatic and non-electrostatic) attraction between chain and surface, and the increase of free

energy of the adsorbed chains due to the loss of configurational entropy. Non-electrostatic interactions play a key role in this balance [79, 81, 82], as also the analysis of the effects of adsorbed polyelectrolytes on the integrity of the double layer of liposomes, developed in section 2, suggests. However, in our discussion, we will focus for brevity on electrostatic coupling, referring the reader to the recent review of Nylander *et al* [73] for a more detailed discussion on the effect of non-electrostatic interactions on polyelectrolyte adsorption.

To describe the coupling of polyelectrolytes to a charged interface bathed by the polymer solution, several theories have been proposed [26, 27, 80, 83–85]. The main questions that have been addressed concern the conformation of the adsorbed molecules and the structure of the layer, and the origin and amplitude of the charge overcompensation, i.e. the possibility that more polyelectrolyte adsorbs than is needed to neutralize the interface (overcompensation), so that the overall net charge of the surface changes its sign (charge inversion).

A key role in this phenomenology is played by the fraction of counterions of the polyelectrolyte that condense along the chain.

In dilute solutions of polyelectrolytes inter-chain interactions are negligible and a ‘cell model’ holds. The volume is divided into unit cells, containing a single polyelectrolyte surrounded by its counterions, with a size of the order of the average distance between the chains. In a very dilute solution, the entropic penalty for the counterion being trapped close to a polyion is very high and virtually all counterions leave the chains, freely diffusing in solution. As the polymer concentration increases, the entropic penalty for counterion localization decreases. As a consequence, a number of counterions ‘condense’ in a small volume close to each polyion. This phenomenon is known as Manning–Oosawa counterion condensation [86–88] (see also [72, 89] and the literature cited therein). In the framework of counterion condensation theory, a parameter of effective charge can be defined as  $\xi = l_B/b$ , where  $b$  is the spacing of the charged groups with valence  $z_p$  along the polyion chain and  $l_B = e^2/(4\pi\epsilon_0\epsilon_r K_B T)$  is the Bjerrum length, i.e. the distance where the electrostatic interaction between two particles with an electric charge  $e$  and suspended in a medium with permittivity  $\epsilon_0\epsilon_r$  reduces to the thermal energy  $K_B T$ . In general, the Manning criterion for counterion condensation  $l_B/b > 1/|z_p z_c|$ , where  $z_c$  is the valence of the counterions, states that when the charge density along the chain ( $e|z_p|/b$ ) exceeds the largest allowed value (i.e. charge spacing  $< |z_c|l_B$ ), counterions condense to decrease the effective charge density to the maximum allowed value.

The counterion fraction that will condense on the polyion chain to reduce its effective charge density is  $1 - f = 1 - b/(l_B|z_c z_p|)$ , so that each polyion bears an effective charge  $Q_p = z_p e N f$ , while the remaining fraction  $f = b/(l_B|z_c z_p|)$  of counterions is (relatively) free in solution.

If a simple electrolyte is added to the suspension, the increased ionic strength screens the electrostatic interactions, influencing the configuration of the polyion chains and the properties of the solution as a whole. For small enough (stoichiometric) charge density, this screening is accurately described by the linearized form of the Poisson–Boltzmann

equation and is quantified by a screening length  $d$  (the Debye length) defined as  $d \equiv \kappa^{-1} = (4\pi l_B \sum z_i^2 c_i)^{-1/2}$ , with  $\kappa$  the Debye screening constant, and where  $c_i$  is the number density of ions of valence  $z_i$ .

The theoretical prediction that the thickness of the adsorption layer formed by a strong polyelectrolyte on an oppositely charged surface in a solution of low ionic strength is proportional to the inverse square root of the charged polymer fraction [90] has been confirmed experimentally [91].

More recently, the dependence of the conformation of the chains, and consequently of the layer thickness, on both the charge densities of the polyelectrolyte and of the surface has been thoroughly analyzed on the basis of the scaling model for flexible, highly charged polyelectrolytes [72, 85].

In a regime of sufficiently low added salt, intra-chain and inter-chain electrostatic interactions strongly influence both the chain conformation and the properties of the solution. This is especially evident in the case of flexible polyelectrolytes. In describing the conformation of these polyelectrolytes the scaling approach is revealed to be very effective [92–94].

Such an approach is based on the assumption of the separation of different length scales and the concept of ‘electrostatic blob’ as the elemental unit of chain conformation. On very small scales (of the order of a few monomers), owing to the insufficient charge repulsion to modify its conformation, the chain forms little coils or ‘blobs’, and inside these ‘blobs’ its conformation is almost unperturbed by electrostatic interactions. Due to the counterion condensation each ‘electrostatic blob’ bears an effective electrostatic charge, but within a blob the chain adopts a conformation consistent with the thermodynamic interaction between uncharged monomers and solvent [72]. In polar solvents and in a dilute solution, a flexible polyelectrolyte with no added salt adopts a highly extended (directed random walk) conformation with a length which is determined by the strong electrostatic repulsion between the electrostatic blobs. As the concentration is increased above a critical value (overlap concentration) the polyelectrolytes maintain their highly extended conformation only up to a characteristic correlation length,  $\xi_c$ , independent of chain length and decreasing as the concentration increases. On larger scales, the chains are random walks of ‘correlation blobs’ (of size  $\xi_c$ ) with an overall chain average size that scales with the polymer concentration. This blob structure remains valid for the adsorbed chains [27].

Polyelectrolyte chains replace counterions at the oppositely charged surface with the charge density  $\sigma$ . For polyions with effective valency  $fN$ , the Gouy–Chapman length [14] is [95]  $\lambda_{GC} = (2\pi l_B f N \sigma)^{-1}$ , and at length scales larger than this length the polyion density decays as the inverse square root of the distance from the surface. Here  $f$  is the fraction of charged monomers (or the fraction of *free counterions*).

For surface charge densities  $\sigma \gtrsim [l_B^2 (fN)^3]^{-1/2}$  the distance between adsorbed chains,  $R$ , becomes larger than their average distance to the surface  $D$  (layer thickness), which is of the order of  $\lambda_{GC}$ . In this regime [95], due to the reciprocal strong electrostatic repulsion, the adsorbed chains tend to organize in a two-dimensional strongly correlated Wigner liquid [96]. Comparing the electrostatic energy of

the adsorption and the electrostatic self-energy of a chain Dobrynin *et al* [95] showed that, as long as polyelectrolyte chains do not overlap in the adsorbed layer, the attraction to the surface does not perturb the internal conformation of the polyelectrolyte chain, which remains determined by the electrostatic repulsion between the charged monomers and the interactions with the solvent, but only affects the translational and orientational degrees of freedom of the chain.

An important corollary of this remark is that, in this regime, the value of the fraction  $f$  of counterions that are not condensed, being determined by the electrostatic blob size, is minimally affected by the interaction with the oppositely charged surface. In other words, within the ‘blob picture’ the polyelectrolytes maintain their condensed counterions when they become adsorbed (see also section 4). Hence, in calculating the effect of the adsorption on the net charge of polyelectrolyte-decorated particles, the effective charge of the polyelectrolyte  $fN$  must be considered.

As a result of the balance between the electrostatic attraction of the chains to the surface and their confinement entropy, the layer thickness  $D$  decreases with increasing  $\sigma$  (chains lie flatter and flatter) as  $D \approx (f\sigma l_B/b^2)^{-1/3}$  (in a  $\theta$  solvent), where  $b$  is the monomer size.

In this regime, at the lowest order in the Debye screening constant  $\kappa$ , the charge of adsorbed polyelectrolytes,  $f\Sigma$  (where  $\Sigma$  is the surface density of adsorbed monomers), compensates the surface charge, i.e.  $f\Sigma \approx \sigma$ . However, at higher order in  $\kappa$ , adsorbed polyions *overcompensate* the surface charge and  $f\Sigma = (\sigma + \delta\sigma)$ . The excess charge  $\delta\sigma$  is due to the presence of loops, as a result of the configurational entropy of the chains, depending on the surface charge density  $\sigma$  as [72, 97]

$$\frac{\delta\sigma}{\sigma} \approx \kappa D(D/D_e)^2 \quad (1)$$

where  $D_e$  is the electrostatic blob size.

As the surface charge density further increases, a value of  $\sigma \equiv \sigma_e = f/b^2$  is reached when the adsorbed polymer chains come into close contact. For  $\sigma > \sigma_e$ , the polymers cannot lie flat at the surface any longer and they form a ‘self-similar carpet’ [72, 95]. The layer thickness  $D$  increases now with  $\sigma$  as  $D \approx D_e(\sigma/\sigma_e)^{1/3}$ . In this ‘carpet regime’, Dobrynin *et al* [27, 72] predict an overcharging

$$\delta\sigma \approx \sigma_e \kappa D_e [1 - \kappa D_e (\sigma/\sigma_e)^{4/3}] \quad (2)$$

that increases with  $\sigma$ . In this regime, the electrostatic attraction between polyelectrolytes and charged surface is not balanced anymore by the confinement entropy of the whole chain, but is the short-range repulsion between monomers that comes into play. At these high values of the surface charge, attraction becomes strong enough to deform the chain on length scales smaller than the electrostatic blob size  $D_e$  and this deformation could affect the value of counterions’ fraction that remain condensed.

As an example of the above sketched picture, for sodium poly(acrylate) [NaPA], characterized by a monomer size  $b \approx 1.8 \text{ \AA}$  [98], the charge fraction  $f$  on the polyion calculated from the Manning theory is  $f \approx 0.25$ , which gives a value of the crossover surface charge density  $\sigma_e$  equal to one elementary

charge  $e$  per  $\approx 13 \text{ \AA}^2$  [82]. Other authors [99], on the basis of different estimates of  $f$  and  $b$ , report for NaPA adsorption a value of  $\sigma_e$  of  $1/50 \text{ \AA}^{-2}$ . In any case, such surface charge densities are higher than the typical values that can be reached in phospholipid layers even when all the component lipids are charged (for example, for a DOTAP lipid film at its maximum compression before the collapse  $\sigma \approx 1/60 \text{ \AA}^{-2}$ ). These considerations suggest that in the case of the polyelectrolyte that decorate charged liposomes the strongly correlated Wigner liquid regime holds rather than the self-similar carpet one.

However, the phenomenology shown by these systems is complex and still there are several aspects that deserve to be carefully investigated. For example, in a similar system (NaPA adsorbed on a dimethyl-dioctadecyl-ammonium bromide, DODA, monolayer deposited at the air–water interface), Hénon *et al* [99] recently reported a different regime for the overcharging as a function of  $\sigma$  (varied by lateral compression of the film) above a crossover charge density  $\sigma_c \approx 1/220 \text{ \AA}^{-2}$ . Also the elastic behavior of the film they observe seems to be consistent with a transition from a flat adsorbed layer to an ‘adsorbed carpet’ above this value of  $\sigma$ . From the measured elastic modulus the authors infer that, below  $\sigma_c$ , the adsorbed polymers form a dense two-dimensional film, which is difficult to compress. Conversely, for  $\sigma > \sigma_c$ , the adsorbed polymers form a ‘carpet’ that is much easier to compress, since now the layer complies with the compression by changing its thickness.

For less flexible polyelectrolytes the blob picture is invalid and the scaling approach has limited application. Applying the Kuhn formalism [93], the conformation of the polyelectrolyte chain can be described in terms of a statistical (Gaussian) chain of  $N_{lk}$  segments of length  $2l_p$  [100], where  $l_p$  is the total persistence length, including the contribution due to the electrostatic repulsion between the charged monomers [101]. Also in this case the counterion condensation occurs when the charge density along the chain exceeds the critical value ( $e|z_p|/b > e|z_c|l_B$ ).

The picture that we have briefly sketched above for the adsorption of flexible polyelectrolyte remains qualitatively valid also for rod-like chains, at least in the regime of sufficiently low charged surfaces where also rigid polyions arrange in a strongly correlated Wigner liquid when they adsorb [28]. For the long and rigid ‘spaghetti-like’ DNA molecules correlations mean local parallel arrangement of the chains, resulting in the typical ‘fingerprint’ patterns [25] also observed on the surface of liposome–DNA aggregates [45]. Conversely, at the larger surface charge densities, instead of a ‘self-similar carpet’ regime, for rigid polyelectrolytes Nguyen and Shklovskii [102] predicted the formation of multilayers, characterized by an oscillating inverted charge.

Although the extent of the overcharging and the details of the ordering of the adsorbed macroions at an oppositely charged surface strongly depend on their geometry (differing for spherical macroions, rod-like or flexible linear polyelectrolytes, etc) the overcharging phenomenon *per se* is very general, depending in the end on the large valence of the macroions or, more explicitly, on the fact that several charged

groups are lumped together on a single macromolecule. The ‘concentration’ of the adsorbed charges in discrete lumps introduces a characteristic length scale associated with the lateral distance  $2R$  between the adsorbed macroions of valence  $Z$  along the plane. A Coulomb coupling constant can hence be defined as  $\Gamma = \frac{(eZ)^2}{\varepsilon R K_B T}$  or, in terms of the characteristic Gouy–Chapman length  $\lambda_{GC}$ ,  $\Gamma = R/2\lambda_{GC}$ . It is worth reminding ourselves what is the interpretation of  $\lambda_{GC}$  within the mean-field theory of Gouy–Chapman. If, on the one hand,  $\lambda_{GC}$  is the distance from the plane where the energy of a  $Z$  ion in the electric field  $2\pi\sigma/\varepsilon$  generated by the charged plane is of the order of the thermal energy ( $\lambda_{GC} = K_B T \varepsilon / 2\pi\sigma Z e$ ), it is also the distance where the  $Z$ -ion concentration,  $N(x)$ , as a function of the distance  $x$  from the plane should drop to one-half, since [14, 28]

$$N(x) = \frac{K_B T \varepsilon}{2\pi (eZ)^2 (x + \lambda_{GC})^2}. \quad (3)$$

It is clear then that in a system which is strongly coupled, because  $Z$  is large, the distance  $R$  between the macroions becomes larger than  $\lambda_{GC}$ . Then, it is not any longer possible to assume each ion is effectively screened on the average by ‘a layer’ of other  $Z$  ions, mean-field treatment along the lines of Poisson–Boltzmann theory fails in this situation, and correlations between macroions cannot be neglected. Perel and Shklovskii (1999) have shown that in this case, i.e. when  $\Gamma \gg 1$ , the screening atmosphere is, in practice, ‘confined’ at the surface and can be approximated as a two-dimensional strongly correlated liquid.

Despite this evidence, charge overcompensation remains a rather counterintuitive phenomenon. Nguyen and Shklovskii suggested an argument that can effectively help in grasping the physics of the overcharging on an intuitive ground. The basic idea is ‘charge fractionalization’ [103, 104]. Let us assume that a charged surface is completely neutralized by oppositely charged  $Z$ -valent polyelectrolyte chains ( $Z$  ions) and that a new polyelectrolyte nears the surface. By forming ‘defects’ at the particle surface, in the form of loops or dangling ends, the adsorbed chains gain some conformational entropy. The charge vacancies left by these defects can be locally large enough to drive the oncoming  $Z$  ion nearer to the surface where, due to the repulsion between the like-charged chains, vacancies can join and enlarge, also allowing the newcomer  $Z$  ion to adsorb, maybe with some loop and ends dangling above the surface. The net result is that, instead of having a  $Z$  ion in the solution, and the surface covered by an ordered array of chains that lay flat on it,  $Z$  disconnected charges appear ‘protruding’ from the polyelectrolyte layer that completely neutralizes the surface. The charge of the polyelectrolyte results in this way ‘fractionalized’ along the surface. This configuration is energetically favored for the system, that gains some conformational entropy of the adsorbed chains and also the self-energy of the  $Z$  ion. This is the energy of repulsion between the  $Z$ -charged groups of the polyelectrolyte in the extended configuration that the chain assumes in the solution. When the same  $Z$  charges are ‘fractionalized’ along the surface they are free to distribute far apart enough so that their

repulsive contribution to the overall energy becomes negligible and the self-energy is hence gained by the system.

Although, as pointed out by Grosberg *et al* [28], correlation is, once again, on the basis of the notion of ‘charge fractionalization’, this concept is also useful to point out that an essential ingredient to produce the correlated adsorption of the  $Z$  ions and, as a consequence, all the resulting phenomenology of the overcharging and of the re-entrant aggregation (see below), is the *mismatch* of the charge modulation patterns on the surface and on the adsorbing macroions. Charge fractionalization (and hence correlation) occurs when multi-valent  $Z$  ions adsorb on a uniformly charged surface, but also when they adsorb on a surface where charges are lumped in discrete groups with valence  $Z_s \neq Z$ . In other words, when a uniformly charged linear polyelectrolyte adsorbs with loops and/or part of the chain dangling above the oppositely uniformly charged surface, or when the distance between the charges along the chain does not match the distance between the charged groups on the surface. In general, the ‘fractionalization’ of the charge appears whenever the distributions of the charges on the surface and on the approaching macroion do not *match*.

Finally, we would stress here (although we will come back to this argument in section 5, where a specific model of inter-particle potential will be presented in detail) that in a system of charged colloidal particles and oppositely charged polyelectrolytes, an attractive contribution to the inter-particle potential could arise from the strong correlation of the polyelectrolyte chains adsorbed at the particle surface.

There is, in fact, increasing evidence, both from experiments [105–109] and numerical simulations [110–118], that in the presence of polyvalent counterions a short-range attraction can be observed between like-charged macroions. Although, despite the great theoretical effort (see, for example, [114, 118] and literature cited therein), a complete description of this counterintuitive interaction is still lacking, there is a general consensus on the essential role that correlations between multi-valent counterions play in the mechanism of like-charge attraction. Multi-valency appears essential in generating strong attractions. In fact, due to dynamic fluctuations, there is always an attractive component, also in the case of monovalent counterions, but in this case the Coulomb coupling  $\Gamma = \frac{(eZ)^2}{\varepsilon R K_B T}$  becomes large enough only in the limit of low temperatures, and at room temperature the Poisson–Boltzmann repulsion dominates [119, 120].

On the other hand, for large enough  $Z$ ,  $\Gamma$  becomes large at relatively high temperatures. In this condition macroions, as we have discussed above, form a Wigner-crystal-like strongly correlated liquid when adsorbed on oppositely charged surfaces. When two of such decorated surfaces oppose and approach each other, showing on the average an identical periodicity (the long-range order of a Wigner crystal is not important for this attractive force [96, 111]), they gain energy by properly positioning themselves in the lateral direction [121]. Intuitively, a short-range attraction arises between the surfaces showing interlocking patterns when a ‘ $Z$ -ion domain’ on one surface corresponds to a ‘ $Z$ -ion-free domain’ on the other one. More quantitatively,

it has been shown that a net attraction arises between two like-charged surfaces immersed in an electrolyte from the non-uniform distribution of the charge ('charge-patch' attraction [32, 122, 123]).

However, independently of the details of the different models for the 'charge-patch' attraction, as has been nicely pointed out by Grosberg *et al* [28], an energetic advantage immediately arise when the two approaching surfaces come so close that their strongly correlated liquids (SCL) merge. In a bi-dimensional Wigner crystal of  $Z$  ions on a neutralizing (plane) surface, the correlation energy gain per ion is proportional to the inverse radius of the Wigner cell  $E \propto -(Ze^2)/R$  [28, 124]. When the two decorated surfaces come in close contact the decorating patterns interlock and each  $Z$  ion is sandwiched between two charged planes. Now the density of the  $Z$  ions doubles and the radius of the Wigner-Seitz cell of the 'merged SCL' is reduced by the factor  $1/\sqrt{2}$ , leading to an energy gain.

Although on a more empirical basis, such mechanisms have already been invoked to justify the aggregating effect of different polyelectrolytes on colloidal particles [105, 107, 125].

#### 4. Electrical transport properties

From the picture outlined in the previous sections, it clearly appears that the correlated adsorption of the polyelectrolyte chains at the colloidal particle surface plays a fundamental role in determining both the phenomena of the 'charge inversion' and of the 're-entrant condensation'. Due to their reciprocal lateral repulsion, polyelectrolytes arrange in two-dimensional, strongly correlated, i.e. showing a defined degree of (short-range) order, 'structures' when they adsorb on the particle's oppositely charged surface. It is this non-uniform distribution that makes possible the overcharging of the colloidal particles, and it is from this surface charge inhomogeneity that 'charge-patch attraction' can arise.

Within this framework, the role played by the small counterions of both the polyelectrolyte and the colloidal particles still remains somewhat controversial. Different authors [49, 70, 126–129] emphasized this role, pointing out that the 'driving force' for the adsorption of polyelectrolytes on an oppositely charged surface could actually be the release of the condensed counterions. However, before discussing this point, the notion of effective charge and counterion condensation for colloidal particles must be defined more precisely in section 4.1.

##### 4.1. The effective charge of colloidal particles

As is well known, in electrolyte solutions, micro-ions accumulate around highly charged macroions, because of the strong electrostatic attraction, which is large compared to the thermal energy  $K_B T$ . As a result, the relevant parameter to compute the electrostatic interactions between the macroions is not the bare charge, but an effective (or renormalized) charge, associated with the 'decorated' object made of the macroion plus its condensed counterions. We have briefly discussed in section 3 the phenomenon

of counterion condensation in polyelectrolyte solutions (Manning–Oosawa condensation [72, 87–89]). A quantitative analysis of the charge renormalization in colloidal suspensions is comparatively more recent, being initiated by the pioneering work of Alexander *et al* in the early 1980s [130]. While in the case of linear polyelectrolytes, which can be modeled as 'charged wires' or cylinders, the counterion condensation is a well-defined concept, its definition in the case of bulky colloidal particles (that in general can be approximately described as irregular spheroids) is more elusive.

In fact, while the dependence of the extent of counterion condensation on the stoichiometric surface charge density of the macroion is plainly apparent, the macroion geometry also plays a role [131].

It is easy to show that, when an isolated charged object is surrounded by an unbounded domain, i.e. at infinite dilution, counterion 'condensation' takes place if the 'object' is a cylinder, but not around a spherical particle. Consider a cylinder of radius  $r$ , uniformly charged with an effective density  $\sigma_{\text{eff}}$  per unit length, the entropy gain when counterions (with valency  $Z$ ) leave the immediate vicinity of the polyelectrolyte moving to a distance  $R$  is  $K_B T \ln(\pi R^2/\pi r^2)$ . However, this costs the energy  $(eZ)(1/2\pi\epsilon_0\epsilon_r)\sigma_{\text{eff}} \ln(R/r)$ . As a consequence, counterions are released only as long as the entropy gain exceeds the energy cost, i.e. as long as  $\sigma_{\text{eff}} < (4\pi\epsilon_0\epsilon_r K_B T)/(eZ)$ . In terms of the Bjerrum length,  $l_B$ , the second member of the inequality is  $e/(|Z|l_B)$  and the Manning condition  $l_B/b_{\text{eff}} < 1/|Z|$  (or  $l_B/b_{\text{eff}} > 1/|Z|$  for condensation) is recovered. The corresponding quantities for a uniformly charged sphere of radius  $r$  and total charge  $Q$  are  $\Delta S = K_B T \ln(R^3/r^3)$  and  $\Delta E = eZQ/(4\pi\epsilon_0\epsilon_r)(\frac{1}{R} - \frac{1}{r})$ , which for  $R$  sufficiently large does not compensate at all, hence some sort of condensation can only occur at finite concentrations. However, also for spheroidal charged particles, the notion of effective charge is widely used in the literature both for the equilibrium and dynamical properties at finite concentrations. Although, as has been pointed out by Belloni [132], it must be noted that the very concept of effective charge becomes less meaningful at high salinities or volume fractions (where the condensed counterion shells overlap) and, obviously, it becomes insufficient and even wrong at high electrostatic coupling.

As a further difficulty, as Taheri-Araghi and Ha [133] have recently shown, a dielectric discontinuity at the particle surface has an influence on the value of its effective charge, in particular, the condensation of monovalent counterions is enhanced. This is typically the case of organic colloids, particularly liposomes, where the dielectric permittivity within the particle is much lower than water permittivity.

In any case, the determination of the extent of charge renormalization of colloidal particles is not straightforward, since it depends on what is the physical property of the counterions which is considered [134, 135], so that often the effective charge is regarded as an adjustable parameter in fitting approximate models to experimental data [136].

A 'natural' way of defining the effective charge of the colloidal particle, known as the 'Alexander prescription' [130, 137], is by asymptotically matching the exact elec-

trostatic potential to the solution of the linearized Poisson–Boltzmann equation. Other criteria [132, 137, 138] commonly used in simulations are the thermal criterion, where the bound counterions are defined as those counterions contained within the radial distance at which the mean electrostatic energy equals the thermal energy, and the concentration criterion, where the bound counterions are those that lie within the distance at which their local concentration equals its average value.

#### 4.2. Counterion release on polyelectrolyte adsorption

The argument in favor of the counterion release as the driving force for polyelectrolyte adsorption on an oppositely charged surface can be summarized as follows. In solution both the polyelectrolytes and the charged surface (of a colloidal particle, for example) are surrounded by their own layer of spatially confined counterions. However, with their net effective charge, the oppositely charged macroions and surface attract each other. Upon approaching, the fixed charges on the macroions and the surface tend to neutralize each other. As a consequence, the confined counterions, not needed any more for the screening of the excess charge, could be released into the bulk solution, thereby increasing their translational entropy. This net gain of entropy would hence represent the ‘driving force’ for the adsorption of the macroions on the surface, and in particular for the complexation of polyelectrolyte and colloidal particles. The adsorption of polyelectrolytes on oppositely charged colloid particles would hence be an ‘entropy-driven’ process.

Such a picture has been invoked for justifying the positive enthalpy changes (endothermic process) observed when DNA complexes cationic liposomes [139–141]. However, these results appear controversial. In fact, since with different liposomes DNA complexation also occurs through an exothermic reaction [141–143], the gain of entropy does not appear as a necessary and distinctive characteristic of the complexation process.

Although different theories show that in the process of adsorption of polyelectrolytes onto a colloidal particle counterions can be completely released [144], mostly released [127], partially released [26], not always released [145] or not released at all (in the case of flexible polyelectrolytes) [27], the possible release of condensed counterions seems to be more a consequence of the adsorption than its cause, for which, as we discussed in section 3.2, correlation is to be credited.

Moreover, considering the counterion release as the ‘driving force’ for the polyelectrolyte adsorption to an oppositely charged surface the overcharging is difficult to justify. As pointed out by Grosberg *et al* [28], assume that a sufficient number of polyelectrolyte chains have already been adsorbed (possibly releasing some or all of their counterions) on a macroion, so that the complex is completely neutralized. Were the  $Z$  ions distributed completely at random on the surface, uncorrelated both in position and orientation or, in terms of ‘charge fractionalization’, were any mismatch of charge densities absent between the surface and the adsorbed polyelectrolytes, the average electric field would be zero. In

this condition, a next arriving polyelectrolyte molecule would have no reason to release its counterions and adsorb.

Besides these considerations, there is now experimental evidence that condensed counterions are not necessarily released by polyelectrolytes upon adsorption on an oppositely charged surface.

Involving different electrostatic parameters, dielectric measurements in appropriate frequency ranges offer valuable information on the distribution of the counterions surrounding charged colloidal particles and on their dynamics [89, 146–148].

By means of electric birefringence measurements Radeva *et al* [9, 36, 149, 150] compared the charge relaxation on polyelectrolytes free in solution or adsorbed on colloidal ferric oxide particles suspended in the same solution, showing that a substantial fraction of condensed counterions remains bound to the polyions when they adsorb onto the particles. By using electrical conductivity methods, electrophoretic mobility and adsorption isotherms, Santore *et al* reached analogous conclusions [151].

Electrical conductivity measurements represent a particularly simple and effective method to obtain an estimate of the extent of counterions released upon adsorption.

By measuring the conductivity of a suspension of charged colloidal particles with increasing amounts of an oppositely charged polyelectrolyte, the peculiar behavior shown in figure 3 is observed.

The excess conductivity, i.e. the difference  $\Delta\sigma = \sigma - (\sigma_l - \sigma_p)$  between the conductivity  $\sigma$  measured for the aggregate suspensions, and the contributions of the pure colloid suspension,  $\sigma_l$ , and that of the pure polyelectrolyte  $\sigma_p$ , shows a marked increase close to the isoelectric point, suggesting a maximum counterion release at this point.

According to Nguyen *et al* [26, 153–155], when linear polyions of radius  $a$  adsorb onto an oppositely charged surface, their effective charge density,  $\eta_{\text{eff}}$ , may be larger than the one they possess when are free in solution,  $\eta_{\text{eff}} = e/l_B$ . Using this notation, the fraction,  $f$ , of the polyelectrolyte counterions that are not condensed has to be written  $\eta_{\text{eff}}/\eta_0$ , where  $\eta_0 = e/b$  is the linear charge on the bare polyion chain. The strong repulsion by the like-charged surface experienced by the counterions condensed on the polyelectrolyte would hence favor a further counterion release upon adsorption. The extent of this release would be governed by two characteristic lengths, the screening length,  $r_s$ , due to the concentration of the small counterions (from both the polyelectrolyte and the oppositely charged surface) in the bulk solution, and the parameter  $A_0 = \eta_{\text{eff}}/\rho_0$ . Here,  $\rho_0$  is the bare surface (stoichiometric) charge density.  $A_0$  can be considered a sort of ‘lateral correlation length’ of the charges on the surface, when  $r_s \ll A_0$ , the polyions do not release their counterions at all, maintaining their effective charge density  $\eta_{\text{eff}}$ . In contrast, with  $r_s \gg A_0$ , the large charge density of the surface forces the polyions to release some of their condensed counterions. It must be noted that, for a given system (i.e. keeping fixed the charge densities on both the particles and the polyelectrolyte) in the case of no salt added, a small value of  $r_s$  can only be realized at very low concentrations (both of the polymer and charged particles).

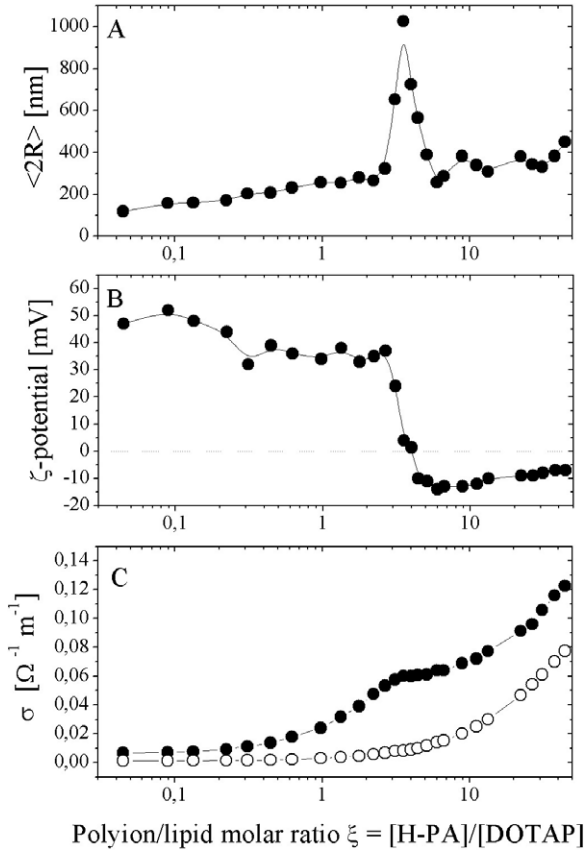


**Figure 3.** The average hydrodynamic diameter  $\langle 2R \rangle$  (A), the  $\zeta$  potential (B) and the electrical conductivity  $\sigma$  (C, (●)) of a suspension of polyelectrolyte-induced liposome aggregates (polyacrylic acid DOTAP) as a function of the polyion to lipid stoichiometric charge ratio  $\xi = C_p/C_l$ . In panel (C) the conductivity of the aggregate suspension (●) is compared with the conductivity of the pure polyelectrolyte solution (○) at the same polymer concentrations. Adapted from [152].

By imposing the appropriate equilibrium conditions for the chemical potential of the ions in the system, for  $r_s \gg A_0$ , the following expression for the linear charge density  $\sigma$  of the adsorbed polyelectrolyte chains can be derived [153, 154]:

$$\eta = \eta_{\text{eff}} \sqrt{\ln(r_s/a) / \ln(A_0/2\pi a)}. \quad (4)$$

In the same conditions the net surface charge density of the complex changes its value from  $q_0$  to

$$q/q_0 = (\eta_{\text{eff}}/\pi a q_0) \exp(-\sqrt{\ln(r_s/a) \ln(A_0/(2\pi a))}). \quad (5)$$

It is then easy to calculate the electrical conductivity  $\sigma$  of a polyelectrolyte-decorated particle suspension at the different polyelectrolyte–particle ratios. Since the contribution of the suspended particles is negligible at the very low volume fractions considered [53], the conductivity of the suspension does not differ appreciably from the conductivity of the dispersing aqueous medium, and assuming the additivity of the contribution of the counterions released by the particles and by the polyelectrolytes, the overall conductivity  $\sigma$ , up to a concentration for which the condition  $r_s \gg A_0$  holds, can be written

$$\sigma = g C_L \lambda_{\text{CiL}} + C_p f \lambda_{\text{Cip}}. \quad (6)$$

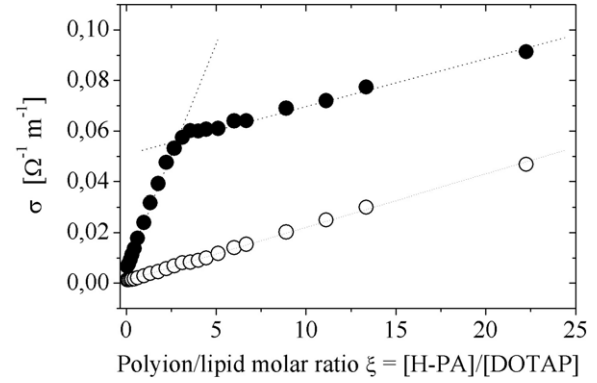


**Figure 4.** On a linear scale, the abrupt change in the linear slope of the electrical conductivity  $\sigma$  (●) measured for complexes of DOTAP cationic liposomes and polyacrylic acid at increasing polyelectrolyte content is even more apparent. The conductivity of the pure polyelectrolyte solution (○) is smoothly linear in the whole range examined. Data from [152].

Here,  $g$  and  $f = \eta/\eta_{\text{eff}}$  are the fractions of free counterions released by the colloidal particles and by the polyelectrolytes,  $C_L$  and  $C_p$  are the stoichiometric concentrations of the counterions (bound and unbound) of the particles and of the polymers, and  $\lambda_{\text{CiL}}$  and  $\lambda_{\text{Cip}}$  their equivalent conductances.

When, at increasing polyelectrolyte concentration,  $r_s$  equals  $A_0$  and, for a further increase, when  $r_s$  becomes smaller than  $A_0$ , the effective charge density of the adsorbed polyions reduces again to the value characterizing the non-adsorbed polyelectrolytes, and in equation (6) the factor  $f = \eta/\eta_{\text{eff}}$  reduces to  $f = \eta_{\text{eff}}/\eta_0$ . As a consequence of the decrease of the extra fraction of free counterions released, from now on, any further addition of polyelectrolyte to the solution contributes a proportionally smaller number of counterions. This effect justifies the change in the slope of the overall conductivity observed in figures 3 and 4.

By using the factor  $g$  in equation (6) as the only adjustable parameter, Cametti *et al* [152] found a remarkably good agreement between the increment in the electrical conductivity  $\Delta\sigma$ , associated with the counterion release measured in their system during the polyelectrolyte-induced liposome complexation, and the increment predicted by this theory.

The abrupt change observed at the isoelectric point in the linear slope of the electrical conductivity measured for the complexes of charged colloids and oppositely charged polyelectrolytes as a function of the polymer/colloid charge ratio (figure 4) can be easily justified also on a more intuitive basis.

To fix ideas, let us assume that the colloidal particles in our suspension bear cationic groups on their surface, so that their small counterions are negative and that the polyelectrolyte we add is anionic, with positive small counterions. Starting with the pure colloidal suspension, suppose adding increasing amounts of the polyelectrolyte. If the particle concentration is sufficiently low, the low frequency electrical conductivity of the suspension will be essentially due to the small ions in solution. Experimentally, we observe that the bulk conductivity of the suspension increases linearly with

the polyelectrolyte concentration, similarly to what happens in a pure polyelectrolyte solution, in the same range of concentrations (figure 4). However, in the presence of the colloidal particles the slope is steeper. In fact, since the polyelectrolyte chains adsorb at the particle surface, when some polyelectrolyte is added to the suspension there are two contributions to the small ion concentration in the bulk. The contribution due to the ‘unbound’ fraction of the polyelectrolyte counterions (which is possibly larger for adsorbed than for free polyelectrolytes, as we discussed above) and a second contribution due to the bound counterions of the particles can be partially released, since part of the surface is now neutralized by the polymer chains. Assuming again the additivity of the different contributions, the conductivity  $\sigma$  can be written as

$$\sigma = gC_L\lambda_{CIL} + C_p f_{ads}(\lambda_{CIL} + \lambda_{Cip}). \quad (7)$$

Here  $f_{ads}$  is the fraction of free counterions of the adsorbed polyelectrolytes, and all the other symbols have the same meaning as in equation (6). In writing this relation the further simplifying assumption has been made that each effective charge on an adsorbed chain sets free just one of the previously bound particle’s counterions. Of course, beyond the point where all the particle’s counterions have been set free, the only contribution remains that of the free counterions of the polyelectrolyte and the conductivity should now be described by the expression

$$\sigma = \sigma_f + C_p f_{ads} \lambda_{Cip} \quad (8)$$

where  $\sigma_f$  is the maximum conductivity reached in the previous regime. Despite the very crude approximations involved, this simple picture apparently takes into account the main features of the observed conductivity behavior, i.e. the linear increase with the polyelectrolyte concentration and the abrupt change of the slope close to the isoelectric point. However, on more quantitative grounds this simple scheme shows its inadequacy. Taking equations (7) and (8) literally, the ratio of the angular coefficients of the two different slopes of the conductivity should be

$$\frac{b_l}{b_h} = \frac{\lambda_{CIL} + \lambda_{Cip}}{\lambda_{Cip}}. \quad (9)$$

In the example shown in figure 4 the counterions are  $\text{Na}^+$  and  $\text{Cl}^-$  for the polyelectrolyte and the particles, respectively. Therefore this ratio, at the temperature of the experiment ( $25^\circ\text{C}$ ), is equal to 2.5 ( $\lambda_{\text{Na}^+}^{25^\circ\text{C}} = 50.1 \text{ S cm}^2 \text{ equiv}^{-1}$  and  $\lambda_{\text{Cl}^-}^{25^\circ\text{C}} = 76.35 \text{ S cm}^2 \text{ equiv}^{-1}$ ), while from the slopes of the two fitted lines a value of 4.2 is obtained. It must be noted, however, that in calculating the ratio in equation (9), the assumption has been made that the fraction of unbound counterions  $f_{ads}$  does not change with polymer concentration and is the same in the two regimes. In contrast, there is some evidence (see, for example, [100] and literature cited therein) that also for polyelectrolytes in solution the fraction of condensed counterions varies with concentration. In particular, for the polyelectrolyte employed in the experiments shown in figure 4, Na-poly(acrylate), in the range of polymer concentrations shown,  $f$  varies from  $\approx 0.6$  to  $\approx 0.1$  [100].

Independently of the details, both the approaches described above lead to the conclusion that counterions are only partially released in the process of adsorption, giving further support to a picture of the phenomenon as governed by the correlation.

## 5. Modeling the inter-particle potential

A fundamental goal in the study of self-assembling structures, like the aggregates that we are considering in this review, is to understand what the inter-particle potential should be in order to obtain that structure. In view of discussing the characteristic of this potential, let us extract, from the above discussion, the main features of the complex phenomenology of re-entrant aggregation observed in these systems, considering, only to fix ideas, the particular case of an anionic polyelectrolyte and of cationic liposomes as the colloidal particles.

As we have discussed in the previous sections, by mixing the two solutions containing the liposomes and the polyelectrolyte, the polymer rapidly adsorbs on the particles’ surface [2] and, owing to the high electrostatic coupling, the adsorbed chains form on this surface a strongly correlated Wigner liquid [28, 72]. As a consequence of the adsorption, part of the counterions condensed on the polyelectrolytes can be released [150, 152–154]. The strong correlation allows the adsorption of more polyelectrolyte chains on each particle than are needed to neutralize its charge, the extent of this overcompensation depending on the structural details of the system (charge density of the surface, linear charge density of the polyelectrolyte, chain flexibility, etc). As a consequence, by increasing the polymer–particle charge ratio, the net charge of the polyelectrolyte-decorated particles decreases at first, passes through zero and increases again in modulus but with the reverse sign, until the maximum allowed overcharging is reached. Beyond this point, the excess polyelectrolyte added to the suspension remains free in solution. It is exactly within this range of polyelectrolyte–lipid charge ratios that the polyelectrolyte-decorated liposomes show a re-entrant condensation forming the long-lived aggregates that we are considering.

As we saw in section 3.2, between two like-charged particles immersed in an electrolyte a net attraction can arise from the non-uniform correlated distribution of the charge at their surface (‘charge patch’) by a sort of electrostatic key–lock mechanism, where the two particles, getting closer, laterally adjust their reciprocal position so that oppositely charged patches on the two surfaces can match, thereby minimizing the energy of the system. In a sense, this mechanism could be described as a sort of bridging, although on a different length scale. However, the distinctive fact of this ‘bridging’ is that, involving the two strongly correlated Wigner liquids on the surfaces, with each polyion bridging between two sides of its Wigner–Seitz cell, it is mediated by the locally ordered arrangement of several adsorbed polyions, and is not due to sparse single chains that independently builds bridges between two particles.

In this context, it is worth noting that the size of the aggregates depends on the polyelectrolyte length. For example,



it has been shown that, close to the isoelectric condition, by varying the ratio of the polymer length to the particle diameter from  $\approx 0.1$  to  $\approx 50$ , the maximum size of the aggregates approximately increases by a factor of four [33, 39]. However, the re-entrant behavior as a function of the polymer–particle concentration ratio is maintained qualitatively identical for all the different polyelectrolyte lengths. Were the aggregation due to a ‘classical’ bridging mechanism one would expect that the *size* of the aggregates depended only on the chain length, and not on both polyelectrolyte length and concentration. This double dependence points out that both these parameters have the same effect of modulating the strength of the attractive–repulsive interactions between the particles. Changes in the polymer concentration both affect the net charge of the polyelectrolyte-decorated particles (thereby affecting the electrostatic repulsion) and the non-uniformity of charge distribution (thereby affecting the charge-patch attraction), while the more strongly correlated liquid formed by longer chains produces an enhanced strength of the charge-patch attraction.

As we have already pointed out, the formation of the stable diffusing clusters observed in different colloidal systems has been justified in terms of a competition between short-range attraction and long-range electrostatic repulsion [16–19]. Being the screened ‘multipole’ attraction due to the charge non-uniformity intuitively characterized by a much shorter range than the screened Coulomb repulsion due to the residual net charge, one could be tempted to interpret also the phenomenology of the re-entrant aggregation observed in polyelectrolyte-decorated particle systems in these terms. Within this scheme, after clusters had grown to a certain size, having accumulated enough charge, they repel additional particles, the maximum cluster size being characterized by the new length scale introduced by the Coulombic long-range repulsion [13, 16–18, 20]. However, for this mechanism to be effective in producing large clusters, the range of electrostatic repulsion should be at least of the same order as the primary particle size (for example, in the system studied by Bartlett *et al* [18]  $\kappa d$  is  $\approx 0.5$ , with  $\kappa^{-1}$  the Debye screening length and  $d$  the particles’ diameter) or larger. Conversely, in aqueous solutions, due to the strong polarizability of the solvent (short Bjerrum length) and the ensuing large screening, this condition is in practice never attained.

Moreover, the repulsive part of the interaction, rather unexpectedly, seems to increase on approaching the isoelectric point. In fact, the normalized second virial coefficient of the aggregates, as measured from static light scattering, shows a re-entrant behavior centered at the isoelectric condition, where it reaches a broad maximum [11]. Rather paradoxically, the quasi-neutral and large aggregates observed in the region close to the isoelectric point seem to repel each other more strongly than the smaller ones, observed when the net charge on the primary pd particles is larger.

This contradiction can be resolved by analyzing the interaction of the primary particles in terms of an inter-particle potential characterized by a potential barrier whose height increases with the size of the aggregates. As we will show, this dependence of the potential, is not an ad

hoc assumption, but descends naturally from the interplay of the screened Coulomb repulsion due to the residual net charge on the pd particles and the attractive components of the inter-particle interaction coming from the non-uniform distribution of the surface charge (charge-patch attraction) and from the ubiquitous van der Waals forces [156]. Moreover, it is consistent with the observed thermal behavior of the aggregates [157], whose size increases with temperature, as expected for a thermally activated aggregation process, where the particles must overcome a potential barrier in order to stick together.

Velegol and Thwar [32] have recently developed an analytical model for the potential of mean force between non-uniformly charged colloidal particles, showing that a non-uniform charge distribution at the surface of the particles results in an inter-particle potential that, even in the case of same-sign charged particles, has an attractive component. The model is based on the Derjaguin approximation and on an extension of the Hogg–Healy–Fuerstenau (HHF) model [158]. It is worth noting that, independently of the nature of the inter-particle potential and as a general rule, whenever the Derjaguin approximation holds the generic force  $F(h)$  between the surfaces of two spheres of radii  $R_a$  and  $R_b$  at a distance  $h$  can be written in terms of the potential  $G(h)$  that would be observed were the two surfaces infinite planes at the same distance  $h$  [159]:

$$F(h) \propto \frac{R_a R_b}{R_a + R_b} G(h). \quad (10)$$

This expression clearly shows that, in these circumstances, the force between two spherical particles increases with their radius, tending toward the limiting force which would be observed for two planes facing each other.

According to Velegol and Twar [32], the pair interaction potential of mean force between two spherical particles ( $a$  and  $b$ ) with a non-uniform distribution of charge on their surface, in units of the thermal energy  $k_B T$ , can be written as

$$\langle \Phi \rangle = \frac{\epsilon \pi R_a R_b}{R_a + R_b} \left[ (\zeta_a^2 + \zeta_b^2 + \sigma_a^2 + \sigma_b^2) \ln(1 - e^{-2\kappa H}) + 2\zeta_a \zeta_b \ln \left( \coth \frac{\kappa H}{2} \right) \right] \quad (11)$$

where  $H$  is the distance between the surfaces of the two approaching particles,  $\epsilon$  the permittivity of the medium and  $\kappa^{-1}$  the Debye screening length.  $\zeta_i$  and  $\sigma_i$  (with  $i = a, b$ ) are the values of the electrostatic surface potentials averaged over the whole surface of the particles and of their standard deviations, respectively.

This inter-particle potential combines a net charge-dependent monopole term (for  $\zeta_i \neq 0$ ), which is repulsive for like-charged particles, and a multipole term, arising from the charge heterogeneity ( $\sigma_i \neq 0$ ), which is always attractive. For non-uniformly and like-charged particles, as is the case of the polyelectrolyte-decorated particles, the two terms, which have a different range, combine to give a global maximum, representing the potential barrier that two approaching particles must overcome in order to stick together.

The height of this maximum and the separation  $H_{\max}$  between the particles' surfaces where the maximum occurs can be easily evaluated from equation (11). For two identical particles ( $R_a = R_b = R$ ) we obtain

$$\Phi_{\max} = \pi \epsilon R \left\{ (\zeta^2 + \sigma^2) \ln \left[ 1 - \left( \frac{\zeta^2}{\zeta^2 + \sigma^2} \right)^2 \right] + \zeta^2 \ln \left[ \frac{2\zeta^2 + \sigma^2}{\sigma^2} \right] \right\} \quad (12)$$

and

$$H_{\max} = \frac{1}{\kappa} \ln \left( \frac{\zeta^2 + \sigma^2}{\zeta^2} \right) \quad (13)$$

respectively. As we have already pointed out, the barrier height increases with the radius of curvature,  $R$ , of the surface of the two approaching particles and, for a given value of the standard deviation  $\sigma$ , increases with the average surface potential (or, roughly, the 'net charge').

This simple picture seems to be able to take into account all the main features characterizing the behavior of re-entrant aggregation observed in the polyelectrolyte-decorated colloidal systems described above. The correlated adsorption of the polyelectrolyte chains on the oppositely charged colloid particles results in a non-uniform distribution of the surface charge. At any given temperature, for a sufficient amount of adsorbed polyelectrolyte the net charge of the primary particles (i.e. the individual pd particles) or, in other words, their average surface potential, becomes low enough to allow the particles to aggregate. Then, assuming that the aggregates also keep interacting through the same potential, but with an increasing effective radius, when this average radius becomes so large that the energy barrier height (equation (13)) exceeds the value of several  $k_B T$ , the aggregation process will stop. This mechanism reproduces the re-entrant aggregation, the observed increase of the size of the aggregates with the temperature for a given polyelectrolyte-particle ratio [157] and the re-entrant behavior of the second virial coefficient [11]. Within this framework the re-entrant aggregation is a direct consequence of the overcharging and of the fact that for increasingly neutral primary particles the aggregate growth stops at larger values of the effective radius. On increasing monotonically the polyelectrolyte-particle charge ratio, the net charge of the particles is progressively reduced at first, and the limiting size of the aggregates increases, but beyond the isoelectric point the polyelectrolyte keeps adsorbing (overcharging), so that the net charge increases again in modulus and the size of the aggregates consequently decreases. Moreover, the observed increase of the size of the aggregates with the temperature is a clear fingerprint of a thermally activated process [82]. Finally, the increase of inter-aggregate repulsions with their effective radius could justify the re-entrant behavior observed for the second virial coefficient [11]. All the peculiar characteristics of the phenomenology observed in pd-colloid systems seem to fit nicely within such a picture.

In order to gain a better understanding of the characteristic of the inter-particle potential of Velegol and Twar and to analyze the phenomenology that this potential could generate, for a more punctual comparison with the experiment, we have

performed some Monte Carlo simulation that will be briefly described in the next section (section 5.1).

Before ending this section let us comment on the assumption that the interaction between the aggregates can also be modeled with the potential (equation (11)) employed for the primary particles, but with a larger effective radius. In general, this assumption can only be valid when the aggregates grow, maintaining an approximately spherical shape. Experimentally, for the aggregates of pd-liposome this condition is reasonably fulfilled. In the case of polyelectrolyte-decorated lipid vesicles, which are rather deformable particles, when a new vesicle sticks on the aggregate, due to the adhesion forces the surfaces in the contact zone appear flattened and the surface tension tends to flatten out the newcomer vesicle on the surface of the aggregate 2, so that in this case a 'drop-like' model for the growth of the aggregates appears particularly reasonable.

Finally, it is worth noting that Nguyen and Shklovskii [160], within a completely different approach, also reached the conclusion that the Coulomb barrier between aggregates of macroions, whose formation is induced by multi-valent counterions, increases with the cluster size. In a different work [104], the same authors point out the possibility that the charge inversion of a macroion due to the adsorption of multi-valent counterions, could occur, at a characteristic counterion concentration, as a first-order phase transition from the undercharged to the overcharged state, the neutral condition being metastable. In other words, within this picture, for the primary particles, let us say the pd-liposomes, the state of zero charge would not be a stable physical state, but the single decorated particle could only exist in states characterized by an excess or deficiency of adsorbed polyions. This hypothesis supports the view of the charge inversion point as a point of instability, where objects pass discontinuously from an incomplete neutralization condition to the overcharging.

### 5.1. Monte Carlo simulation and the thermal activated process

In order to gain some insight into the processes governing the re-entrant condensation behavior in pd-colloid suspensions we explored, by means of Monte Carlo simulations, the interesting phenomenology that can be derived from the mean force potential proposed by Velegol and Twar and described in the previous section (equation (11)) [156]. In these simulations, carried out using a local Metropolis algorithm at room temperature,  $N_p = 10^4$  particles with a diameter  $\langle 2R \rangle = 80$  nm are placed in a cubic box at a relatively low packing fraction ( $\phi = 0.01$ ), varying both the surface potential  $\zeta$  and its variance  $\sigma^2$  to reproduce typical experimental conditions. As we have pointed out above, the compactness of the clusters that form in pd-liposome suspensions justifies the use of a 'capillarity approximation' (see, for example, [161] and the literature cited therein) to simplify the aggregation events. Within such an approximation the aggregation of two smaller clusters, considered as 'droplets' with uniform density, is modeled as an 'oil drop-like' fusion process, where the resulting aggregate retains a spherical shape and the new radius

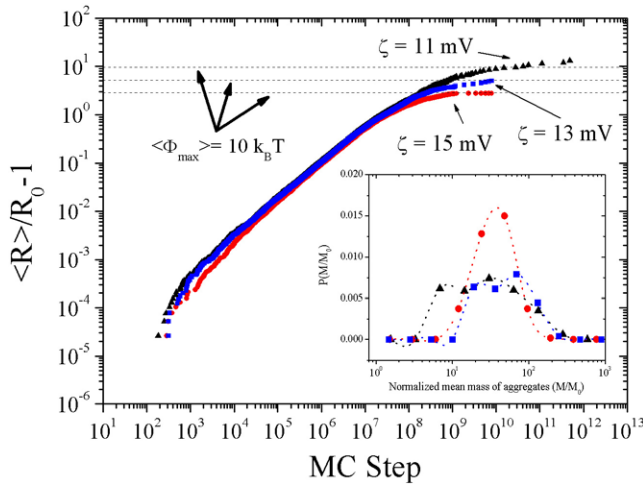


**Figure 5.** Typical MC-step evolution of normalized mean cluster radius  $\langle R \rangle / R_0 - 1$ . Simulations have been carried out for different values of  $\zeta$  potential with a constant value of the standard deviation  $\sigma = 15 \text{ mV}$ . The inset shows the corresponding mass distributions at the plateau. Adapted from [156].

is determined by the condition of mass conservation. As a further assumption, the size of the uniform potential regions on the particle surface (i.e. the size of the charge ‘patches’) is assumed to be independent of the cluster size. To incorporate a Brownian dynamics in the MC algorithm, the  $i$ th particle is selected with a probability which is inversely proportional to its radius (in terms of the primary particle’s radius).

In all the simulations, after an initial transient regime, the radius of the clusters increases, then the growth slows down and the size of the aggregates reaches a limiting value that depends on the electrical surface parameters  $\zeta$  and  $\sigma$ . Figure 5 shows the typical MC-step evolution of the normalized mean cluster radius for different values of these parameters.

The figure clearly shows that, with a constant value of the surface charge non-uniformity (as measured by  $\sigma^2$ ), the plateau is reached at higher values of the mean cluster size when the surface potential decreases. In any case, this plateau is attained when the mean value of the potential barrier height is approximately equal to  $10k_B T$ . As expected, the slowdown of the aggregation dynamics and its arrest is controlled by a mechanism of ‘thermal stabilization’. It must be noted that for decreasing values of the average surface potential of the primary particles the standard deviation of the mass distribution of the aggregates at the end of the process increases significantly. This effect is due to the influence of the particle size on the inter-particle potential and particularly on the barrier height [156], and could justify the broadening of size distributions of the aggregates which are observed experimentally close to the isoelectric point.

The effect of the temperature on the size of the aggregates is considered in figure 6.

The average radius of the aggregates (at the plateau) is plotted as a function of the average surface potential  $\zeta$  for different temperatures in the range from 278.16 to 353.16 K (data from [156]). The inset in the figure shows the variation of the limiting size of the aggregates obtained

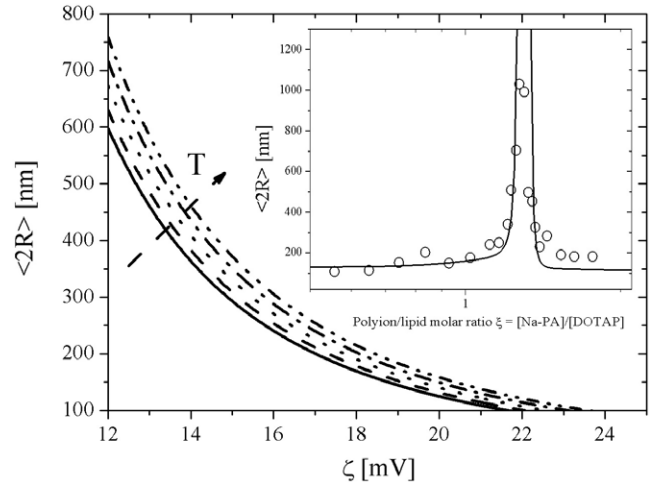


**Figure 6.** Influence of the temperature on the mean cluster size  $\langle 2R \rangle$  as a function of the average surface potential  $\zeta$  and at  $\sigma = 15 \text{ mV}$ . Temperature varies from 278.16 to 353.16 K. Inset: the limiting size that the aggregates reach at the plateau as the  $\zeta$  potential is varied. The line is calculated from equation (12) assuming  $\Phi_{\text{Max}} = 10K_B T$ . Adapted from [156].

from the simulations for different values of the  $\zeta$  potential, consistent with the typical re-entrant condensation observed experimentally; the line is calculated from equation (12) assuming  $\Phi_{\text{Max}} = 10K_B T$ . These results are also consistent with the observed increase of the size of the aggregates formed by pd-liposomes when the temperature is raised [157]. An example of this behavior is shown in figure 7 for DOTAP-polyacrylate aggregates.

Remarkably, when the re-entrant condensation curves observed at increasing temperatures are normalized for this parameter (figure 8), according to equation (12) the data collapse on a single master curve. To obtain this result the different experimental series have been only slightly translated horizontally in  $\xi$  to have the peaks superimposed, but there are no adjustable parameters.

The full line shown in figure 8 is calculated from equation (12) assuming  $\Phi_{\text{Max}} = 10K_B T$ , a linear dependence of the surface potential  $\zeta$  on the polyelectrolyte/lipid charge ratio  $\xi$  and a Gaussian dependence on  $\xi$  of the surface potential non-uniformity parameter  $\sigma$ . Very close to the isoelectric point, data fail to collapse onto the master curve, owing to large fluctuations of the cluster size that could be the sign of a phase transition.

### 5.2. A step further

As we have shown in the previous sections, modeling the inter-particle interactions by means of the Velegol potential (equation (11)) allows us to reproduce semi-quantitatively the main features of the re-entrant condensation phenomenology observed in polyelectrolyte-decorated colloid systems. In equation (11) the ubiquitous van der Waals (vdW) interactions are not considered. It is easy to show that at the low concentrations usually employed in experiments and in the absence of added salt, the Debye screening length, and hence

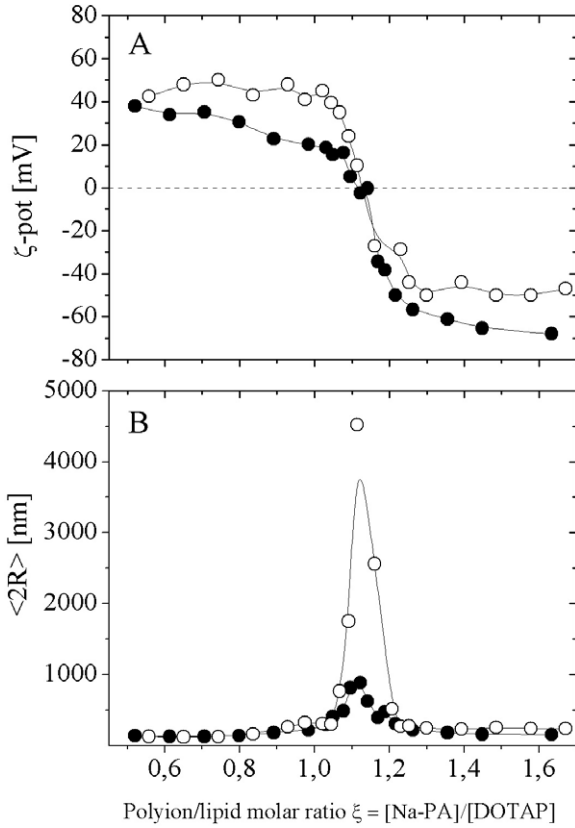


**Figure 7.** Charge inversion (panel A,  $\zeta$  potential) and re-entrant condensation (panel B, aggregate diameter ( $2R$ )) of cationic DOTAP liposomes in the presence of the anionic NaPA polyelectrolyte. Data are shown as a function of the polyion–lipid molar charge ratio,  $\xi$ , for two different temperatures, 80 °C (empty symbols) and 5 °C (full symbols). Lines connecting experimental data are a guide for the eyes only. Adapted from [157].

the range of electrostatic interactions, is so large that the addition of a short-range vdW attractive term in equation (11) does not change appreciably the qualitative picture sketched above [11]. However, for high enough ionic strength of the solution, when the screening length  $\kappa^{-1}$  in equation (11) becomes comparable with the interaction range of the vdW forces, their contribution cannot be neglected any more.

By using the Derjaguin approximation, consistent with the assumptions made in deriving the Velegol expression, van der Waals interactions can be described, in the case of liposomes, by the expression [162]

$$\Phi_{\text{vdW}}(H) = -\frac{AR_aR_b}{6(R_a + R_b)} \left( \frac{1}{H + h_a + h_b} - \frac{1}{H + h_a} - \frac{1}{H + h_b} + \frac{1}{d} \right) - \frac{A}{6} \ln \left[ \frac{H(H + h_a + h_b)}{(H + h_a)(H + h_b)} \right] \quad (14)$$

valid for shelled spheres with radii  $R_i$  ( $i = a, b$ ) and shell thickness  $h_i$  ( $i = a, b$ ) and  $H$  is the distance between their surfaces.  $A$  is the Hamaker constant, whose typical values in the case of liposomes range from  $\approx 10^{-21}$  to  $\approx 10^{-20}$  [163–165]. By adding such a term to the Velegol potential, the inter-potential (assuming the shell thickness

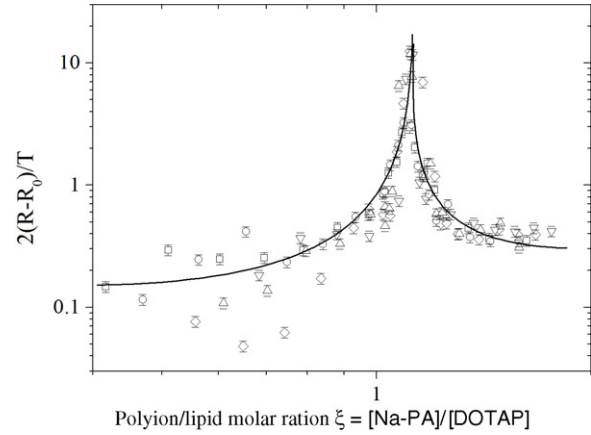


**Figure 8.** The re-entrant condensation behavior of DOTAP–NaPA aggregates observed at different temperatures in the interval from 281 to 356 K (5–80 °C) can be reduced to a single master curve, consistent with the prediction of equation (12). ( $\square$ )  $T = 281$  K; ( $\circ$ )  $T = 296$  K; ( $\triangle$ )  $T = 316$  K; ( $\nabla$ )  $T = 336$  K; ( $\diamond$ )  $T = 356$  K; full line is calculated from equation (12) assuming  $\Phi_{\text{Max}} = 10K_B T$ . Adapted from [157].

identical for all the vesicles,  $h_i \equiv h$ ) becomes

$$\langle \Phi \rangle = \frac{\epsilon \pi R_A R_B}{R_A + R_B} \left[ (\zeta_A^2 + \zeta_B^2 + \sigma_A^2 + \sigma_B^2) \ln(1 - e^{-2\kappa H}) + 2\zeta_A \zeta_B \ln \left( \coth \frac{\kappa H}{2} \right) \right] - \frac{AR_A R_B}{6(R_A + R_B)} \times \left( \frac{1}{H + 2h} - \frac{2}{H + h} + \frac{1}{d} \right) - \frac{A}{6} \ln \left[ \frac{H(H + 2h)}{2(H + h)} \right]. \quad (15)$$

Figure 9 shows the evolution of the pair potential described by this equation when the ionic strength of the solution is increased (i.e. increasing the screening parameter  $\kappa$ ) for realistic values of the parameters involved ( $a = b$ ;  $R_i = 100$  nm;  $\zeta_i = 25$  mV;  $\sigma_i = 15$  mV;  $A = 10^{-20}$  J;  $T = 298$  K).

While at low ionic strength van der Waals interactions can be neglected and the aggregation process is tuned by the energy barrier only, above a well-defined ionic strength, a secondary minimum appears, modifying the aggregation kinetics and the thermodynamic stability of the dispersion. At even higher ionic strengths the repulsive barrier completely disappears, there is only one deep minimum, and the colloid is completely destabilized.

Interestingly, as is shown in figure 10, the increase of the effective radius of the aggregates not only makes the potential barrier higher and higher, as has already been noted (equation (12)), but also deepens the secondary minimum. As a consequence, when this secondary minimum becomes deep enough (several  $K_B T$ ), i.e. for large enough aggregates, particles do not need any more to overcome the potential barrier to stick irreversibly in the primary minimum, but the aggregation occurs in the secondary minimum. In this way the stabilizing effect on the growth of the aggregates due to the increase of the potential barrier with their radius is lost and the clusters keep growing until, ultimately, they separate in phase (flocculation).

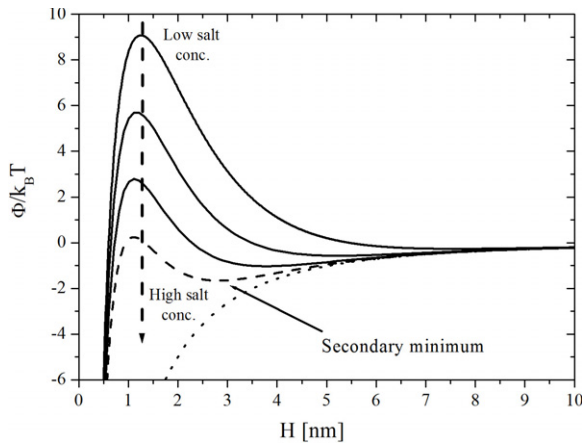


**Figure 9.** The evolution of the pair potential described by (15) obtained by adding a van der Waals term to the Velegol potential of equation (11) when the ionic strength of the solution is increased. At low ionic strength van der Waals dispersion interactions can be neglected and the aggregation process is only tuned by the energy barrier that the approaching particles must overcome to stick together. Above a well-defined ionic strength, a secondary minimum appears. At higher ionic strength the repulsive barrier disappears and there is only one deep minimum. The screening parameter  $\kappa$  varies from  $0.5 \text{ nm}^{-1}$  (full line) to  $3 \text{ nm}^{-1}$  (dotted line). The effect of the screening on the dispersion forces [166] has been neglected.

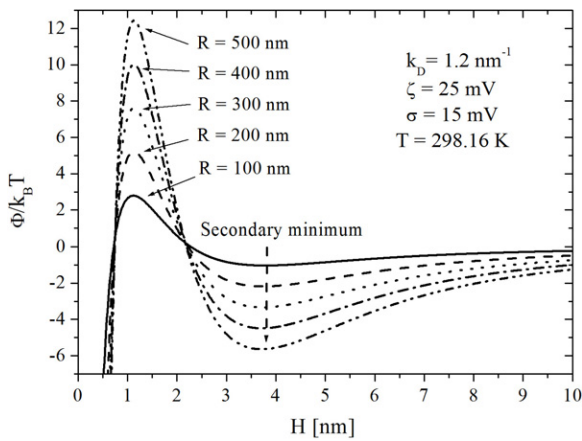


**Figure 10.** Effect of the clustering on the inter-particle potential of equation (15) that, besides taking into account the screened electrostatic repulsion and the effect of the surface charge non-uniformity, also considers the van der Waals dispersion attraction. As far as the radius of the particles increases, the potential barrier height increases as usual (equation (13)) but now also the secondary minimum deepens.

The predicted behavior is consistent with what is observed experimentally when a simple electrolyte is added to a pd-liposome solution.

In a pd-liposome solution with no added salt, the ionic strength contributing to the electrostatic screening, which is due to the free counterions only [167], can be roughly estimated from the known polyelectrolyte/particle concentration, assuming a reasonable value for the fraction of free counterions. For a sufficiently diluted suspension (particle volume fraction of the order of 0.01) the screening

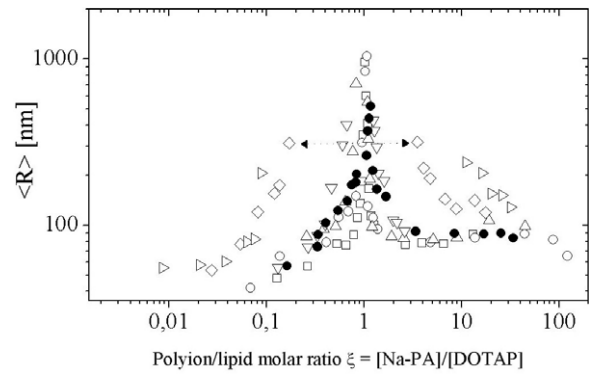


**Figure 11.** Average radius,  $\langle R \rangle$ , of polyelectrolyte-decorated liposome aggregates (NaPA–DOTAP) as a function of the polyelectrolyte/lipid molar charge ratio,  $\xi$ , in the presence of different concentrations of a simple electrolyte (NaCl): (●) 0.5 M; (◇) 0.4 M; (▽) 0.3 M; (△) 0.1 M; (○) 0.05 M; (□) 0.005 M; (●). As an example, the arrows mark the width of the zone of instability for 0.4 M NaCl.

parameter  $\kappa$  can be typically as low as  $0.2 \text{ nm}^{-1}$ . In this condition the secondary minimum should not exist and the aggregation should be governed by the potential barrier. In fact, the aggregation behavior which is observed experimentally in this case shows the typical features of a thermally activated irreversible aggregation [157]. However, by adding some simple salt to the suspension, the observed phenomenology changes significantly (figure 11). Not only, as could have been easily predicted, due to the increased screening much larger aggregates form for the same polyelectrolyte/particle ratio (i.e. for the same value of the residual net charge on the pd particles) but, above a given concentration of the added simple salt, the observed behavior changes qualitatively. Now, the characteristic finite-size aggregates can only be observed far away enough from the isoelectric condition, i.e. for sufficiently high values of the residual net charge on the primary particles. But there is a whole interval of the polyelectrolyte/lipid charge ratio  $\xi$  centered on the isoelectric point where the finite-size aggregates are not observed and the liposome suspension is simply destabilized by the addition of the polyelectrolyte. Notably, this interval widens with increasing salt concentrations.

Assuming for the inter-particle potential the expression given by equation (15) this peculiar behavior finds a simple interpretation. For a given ionic strength of the solution, a limiting value of the average surface electrostatic potential (in absolute value) can be determined. Above this value (i.e. when electrostatic repulsion is still sufficiently strong), as the radius of the aggregates increases, a height of the potential barrier sufficient to prevent any further growth (several  $K_B T$ ) is reached before the secondary minimum becomes deep enough for driving the aggregation. Conversely, below the critical value (i.e. sufficiently close to the neutrality condition) before a sufficient height of the barrier is build up by the radius increase, the secondary minimum is already deep enough to dominate the aggregation process and the suspension results completely destabilized.

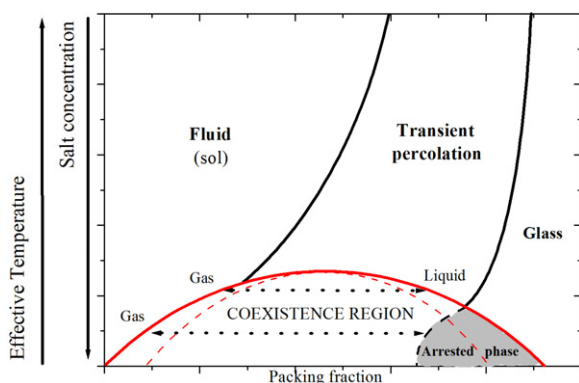


**Figure 12.** Phase diagram for a generic short-range interacting particle. The addition of salt acts as a thermal quenching of the system, up to a ‘critical’ concentration, into the two-phase region. The process may lead to an arrested denser phase. It is not clear yet how the glass line continues within spinodal region (dashed line). Adapted with changes from [169].

From a more general point of view, the addition of the salt is in practice equivalent to lowering the effective temperature of the system. In systems where, as in this case, a secondary minimum appears, this reduction of the effective temperature can induce, in principle, a thermodynamic instability, leading to a phase separation into a poor and rich colloid region [13, 168] (see figure 12). In this case, an intriguing possibility is that, by crossing a glass transition boundary, the denser phase becomes arrested, a phenomenon that has been recently hypothesized as a ‘non-equilibrium’ route to gelation [168, 169].

Preliminary results show that for polyelectrolyte-decorated liposome suspension, in the instability region where the addition of the salt prevents the formation of the characteristic finite-size aggregates, two different populations of suspended particles can be observed, as shown by dynamic light scattering experiments.

The average size of the smaller particles, which remain stable in time, is slightly larger than the primary particles and they could be identified as the ‘stabilized clusters’ at that effective temperature (salt concentration). The size of the second particle population rapidly increases in time, resulting in the instability which is observed macroscopically. The hypothesis that this phenomenology could be interpreted in terms of a phase separation and of a resulting arrested state appears intriguing. However, much experimental work is needed to substantiate such a picture, in particular the region of higher volume fractions should be carefully explored.

## 6. Possible biomedical applications: developing a new class of vectors for multi-drug delivery

With the impressive progress in molecular biology, genetic therapy appears as a therapeutic modality with a tremendous potential impact on the quality of human life. In this therapeutic modality genetic material is delivered to the interior of specific target cells of the organism. In the more traditional approach, properly termed gene therapy, a gene of

interest (a DNA fragment) is inserted into the genetic code to restore or correct some function in the cell. In a rapidly developing different approach (the so-called ‘RNA silencing’ technique) small non-coding RNA molecules are delivered to the cell cytoplasm that, on the basis of different mechanisms not yet completely understood [170], can specifically inhibit the expression of pathogenic genes (see, for example, the recent monographic supplement to the journal *Nature* on these topics [171]). In both cases, a proper *vector* is needed to transport the therapeutic nucleic acids through the cell membrane, delivering them to the cytoplasm. Unfortunately, in spite of the clinical interest, the frustrating inadequacy of the different vectors that have been employed so far strongly impairs the efficacy of these therapeutic approaches.

In general, in order to reach their target, all drugs have to be transported through the complex ‘aqueous environment’ which is a living body, crossing a series of different ‘barriers’ [172]. For example, in the case of the genetic material to be transported into the cell nucleus, being both DNA and RNA polyelectrolytes, the main obstacle is the cell membrane, whose hydrophobic core presents a formidable barrier to the passage of charged molecular species. On the other hand, many effective drugs are hydrophobic or amphiphilic since their natural targets are membranes or membrane-bound receptors. In this case, the ‘barrier’ is represented by the difficulty of transporting these water-insoluble substances through the blood stream or the extracellular fluid. Moreover, drugs are often easily deactivated by the enzymes of the body fluids, or are toxic for healthy tissues. Finally, even if the drug is able to cross the necessary barriers without being degraded and without producing undesired side effects, it is still possible that, having reached its target, its local bio-availability is not sufficient for effective pharmacokinetics. In all these cases the active substance must be encapsulated in a proper vector, for protection, effective transport and/or reduction of its toxicity.

A major goal in drug delivery is hence the ability of designing vectors that, exploiting some natural pathway (endocytosis), or being able to fuse with the cell membrane, can deliver their ‘bio-active payload’ to a particular target organ or tissue or directly inside a malfunctioning cell.

Viruses have naturally evolved to efficiently infect eukaryotic cells, transferring their genetic materials into the host cell. Different viruses have been evaluated as possible carriers for gene therapy, but they have proved of limited use, particularly owing to the significant risks of toxicity and/or immunogenicity that make their acceptance by the patients generally low [173, 174].

Synthetic non-viral materials, such as cationic lipids and polymers, mineral particles and lipid assemblies, are rapidly gaining popularity as vectors for delivering genes and other macromolecules to target organs and cells. Although currently less efficient than their viral counterparts [175], non-viral vectors are under intense investigation as a safer alternative [173, 174]. These vectors have several potential advantages compared to viral systems, including lower toxicity and immunogenicity, simpler quality control and regulatory requirements, and lower limitation in the size of the material to be transported.

For successful delivery, a non-viral vector must be able to overcome many different barriers, to protect its payload and deliver it as specifically as possible, for an efficient expression of its action in target cells. Different strategies aimed to obtain these ideal performances are currently being investigated, being based on employing the peculiar characteristics of different classes of nanostructured materials: bio- and synthetic polymers (particularly star polymers), mineral particles and lipid assemblies.

Among these, the strategy based on the supra-molecular structures formed between charged polymers and oppositely charged particles, particularly liposomes, shows promising potential. The main advantage of these supra-molecular assemblies resides in their intrinsic modularity and flexibility.

### 6.1. Polyelectrolyte–colloidal particle assemblies as multi-compartment vectors for multi-drug delivery

The long-lived finite size of colloidal particles ‘glued together’ by oppositely charged polyelectrolytes shows an interesting potential for developing a new class of multi-compartment vectors for the simultaneous delivery of different pharmacologically active molecules.

In their different compartments, each one formed by an individual primary particle, a decorated vesicle, the aggregates can host different substances [1, 41]. Due to this multi-compartment structure, a single nano-aggregate would hence be able to transport, separately but simultaneously, and to deliver to a single cell, different active substances, including for example, beside the required drugs, also diagnostic probes for the direct ‘real-time’ visualization of the effective drug transfer and downstream processes.

The procedure for assembling these multi-compartment vectors is straightforward in principle. Different charged colloidal particles, for example ionic liposomes differing in composition and/or payload, can be prepared separately and then mixed in solution in the proper proportion to obtain the desired stoichiometry of the various transported components. Then, the aggregation process is initiated by adding the oppositely charged polyelectrolytes that induce the formation of the multi-liposome clusters. For large enough clusters, a defined stoichiometry of the different components established in the suspension is reproduced within each aggregate. In this way, by controlling the stoichiometry at the nanoscale, it can be reasonably assumed that each of the different substances to be delivered will reach any single cell.

This peculiar aspect is particularly appealing in developing new strategies in anti-retroviral therapies. In the last few years, several biological and non-biological carrier systems have been developed for anti-HIV therapy. Among these, liposomes showed an excellent potential and have been tested with various drugs [176, 177]. Generally, large nanoparticles are cell-specific transporters of drugs against macrophage-specific infections such as HIV. Macrophages are the cells of the immune system specifically in charge of the capture and destruction of ‘foreign particles’ (cellular debris and pathogens) in tissues by ingesting (phagocytosis) and enzymatically degrading them. But macrophages are also an elective reservoir for the

HIV virus that is difficult to penetrate by using the traditional pharmacological approaches [178]. Moreover, the HIV virus is characterized by extreme genetic variability and a high mutation rate that allows for rapid escape from adaptive immune responses [179]. For this reason ‘cocktails’ of different drugs potentially active against the different strains of the virus are usually employed in therapy. In this case, there is hence a strong practical advantage in using a multiple vector, able to deliver all the components of the cocktail to any single macrophage cell.

Besides charged liposomes, different colloids can be employed, polymeric nanocapsules for example, or different nanostructured polymers that are already employed as drug carriers (chitosan nanoparticles [38], for example). However, by employing liposomes as the colloidal particles, the huge potential of these versatile lipid assemblies as drug carriers [180] can be fully exploited.

Lipid vesicles have long been studied as systems that could furnish an effective solution to the problem of encapsulation, transport and delivery of pharmacologically active molecules to cells and tissues.

In his interesting book *Life—as a Matter of Fat*, Mouritsen writes: ‘First of all, lipids are amphiphiles designed to mediate hydrophobic and amphiphile environments, which makes them perfect emulsifiers. Secondly, many lipids are bio-compatible and biodegradable and hence harmless to biological systems. Thirdly, lipids are a rich class of molecules allowing for a tremendous range of possibilities. Finally and possibly most important, lipids are the stuff out of which the barriers that limit drugs transport and delivery are themselves made. Therefore by using lipids for transport and delivery of the drugs, one can exploit nature’s own tricks to interact with cells, cell membranes, and receptors for drugs [172]’.

A further advantage of the structures formed by lipid molecules for their biotechnological use is that they form spontaneously by ‘self-assembly’. The concept of ‘self-assembly’ dates back to the observation that, in proper conditions, the proteins and the RNA components of the tobacco mosaic virus could spontaneously re-assemble in solution into active virus particles [181, 182]. Molecular self-assembly at equilibrium is central to the formation of biological structures. It is through the hierarchical self-assembly of simpler bio-molecules that very complex structures such as the cell organelles are built up. The mechanisms at the basis of the hierarchical organization are determined by competing molecular interactions (hydrophobic/hydrophilic interactions, hydrogen bonding, van der Waals, screened attractive/repulsive electrostatic interactions, etc) and entropy effects. A cascade of bond strengths and molecular interactions produces a hierarchy of characteristic lengths at the molecular level and this is reflected in a structure of the final assembly which is determined on the nanometer scale [183, 184].

In principle, by exploiting the self-assembly ability of bio-molecules the geometry and the characteristics of the vectors to be employed in drug delivery could be controlled at the molecular scale.

As an example of this strategy, to overcome one of the major drawbacks in the use of liposomes as drug vectors,

i.e. their liability to be captured and destroyed by the immune system cells when injected into the blood stream, 'stealth liposomes' have been designed that are screened from the macrophages by a polymer coat. This coat is simply build up by incorporating a certain amount of polymer-grafted lipids in the lipid mixtures from which the vesicles self-assemble.

Many of the interesting features of the variously modified liposomes could in principle be transferred to their polyelectrolyte-induced 'multi-compartment' aggregates. 'Conventional' liposomes have been modified in different ways to improve the efficient transfer of their payload to the cell cytoplasm. For example, by using hybrid niosomes as the primary particles forming clusters [41], the characteristics of 'stealth carriers' of these vesicles are transferred to their aggregates. Hybrid niosomes are build up with a mixture of pegylated lipids (e.g. Tween20) and cholesterol, plus a ionic lipid (phosphatidic acid or dicetylphosphate), to confer the desired net charge to the vesicles. The presence of the poly(ethylene glycol) moieties at the particle surface is very effective in reducing undesired interactions with the extracellular environment, with the result of a prolonged circulating lifetime [185, 186] of these 'polymer-shielded' particles. As another example, it has been very recently shown that decorating the liposome surface with the oligopeptide octa-arginine greatly enhances their cellular uptake, and that by optimizing the density of the peptide and its surface distribution, the liposomes could be internalized via clathrin-independent pathways, a mechanism that improves the intracellular trafficking, avoiding lysosomal degradation [187]. The possibility of obtaining multi-compartment clusters of octa-arginine liposomes is currently under investigation in our laboratory.

Besides the ability to deliver different substances separately but simultaneously, the multi-compartment structures formed by polyelectrolyte-decorated liposomes also show other potential advantages.

Supra-molecular hydrogels based on the self-assembly of complexes between various bio-macromolecules are actively researched in view of their use as implantable drug delivery systems for sustained and controlled release of macromolecular drugs [188]. In general, scaffolds serve a central role in many technological strategies by providing the means to control the local environment. Moreover, scaffolds also provide the means of prolonging the release of active macromolecules simply by trapping them within a matrix that delays their delivery to the surrounding environment.

The multi-compartment clusters formed by pd-liposomes, or pd-nanostructured polymers, could in principle work as nanoscaffolds, offering the possibility of extending the duration of the release period of the different substances enclosed in their compartments. Water-soluble active substances, for example, entrapped within the aqueous core of the compartments will be released to the surrounding aqueous medium only progressively, as the degradation and the rupture of the single vesicles proceeds from the more external compartments towards the interior of the cluster. In fact, the pd-liposome cluster could serve simultaneously as a multi-load cargo, transporting several different drugs

and/or diagnostic probes, a protective envelope and incubator, shielding the active substances from the aggression of the degrading enzymes of the extracellular fluids and maintaining the proper 'nano-environment' for the drug storage, and a controlled release dispenser.

## 7. Conclusions and perspectives

Polyelectrolyte-decorated colloid particles and the mesoscopic clusters they form should be regarded as a new class of colloids, both for the intriguingly new phenomenology they show and for their potential for biotechnological applications. Due to the growing interest that these systems have attracted in the last few years, several aspects of their peculiar behavior have been clarified. There is now sufficient experimental evidence that the finite-size clusters that are observed in these systems are not equilibrium aggregates but rather metastable long-lived structures.

Interestingly, the size of these clusters would be stabilized by the presence of a barrier in the inter-particle potential, whose height depends on the radius of curvature of the approaching particles, on their net electrostatic surface potential (in other words, on their residual net charge) and on the non-uniformity of the charge distribution on their surface.

The peculiar re-entrant condensation observed in these systems, with the size of the long-lived aggregates that increases with the polyelectrolyte/particle charge ratio, reaches a maximum close to the isoelectric point and then decreases again when the primary particles are progressively *overcharged*, can be justified in terms of correlated adsorption of the polyelectrolyte chains on the surface of the particles.

In fact, at low enough ionic strength, the height of the stabilizing potential barrier is modulated by the average value of the electrostatic potential and by the non-uniformity of the charge distribution on the particles' surface. Hence, the maximum size reached by the clusters and their residual net charge is controlled by the *correlated* adsorption of the polyelectrolyte chains on the particles.

At higher ionic strengths, the phenomenology becomes more complex. Now a zone of instability appears, centered on the isoelectric point. This instability is probably due to the effect of the ubiquitous van der Waals interactions whose range becomes comparable, at these ionic strengths, to the range of electrostatic interactions. Actually, this further contribution results in the presence of a secondary minimum in the inter-particle potential, whose depth increases with the radius of the aggregates, which could justify the observed instability. Experimentally, there is some evidence that in these conditions two different populations of clusters can form. An intriguing possibility is that by adding some salt a phase separation is induced and that, by crossing a glass transition boundary, the denser phase becomes arrested. Such a phenomenon has been recently hypothesized as a 'non-equilibrium route to gelation' and if only for this reason these systems would deserve further investigation.

However, as we have briefly discussed, the bio-compatible multi-compartment nanostructures that can be, in principle,



easily assembled based on the polyelectrolyte-induced aggregation of oppositely charged colloidal particles apparently have a high potential for biotechnological applications. Multi-compartment vectors based on polyelectrolyte-liposome clusters could be employed for the *simultaneous* delivery of different active substances, drugs, pharmacological or immunological adjuvants, diagnostic probes, etc, to a single cell, and this possibility opens interesting perspectives for developing innovative therapeutic and/or vaccinal strategies.

## Acknowledgments

Sincere thanks are due to Professor Cesare Cametti for stimulating discussions that encouraged the development of ideas for the work that has been reviewed here.

## References

- [1] Bordi F, Cametti C, Sennato S and Diociaiuti M 2006 *Biophys. J.* **91** 1513–20
- [2] Volodkin D, Ball V, Schaaf P, Voegel J and Mohwald H 2007 *Biochim. Biophys. Acta* **1768** 280–90
- [3] Bordi F, Cametti C and Sennato S 2005 *Chem. Phys. Lett.* **409** 134–8
- [4] Raspaud E, Chaperon I, Leforestier A and Livolant F 1999 *Biophys. J.* **77** 1547–55
- [5] Wang Y, Kimura K, Dubin P L and Jaeger W 2000 *Macromolecules* **33** 3324–31
- [6] Bordi F, Cametti C, Diociaiuti M, Gaudino D, Gili T and Sennato S 2004 *Langmuir* **20** 5214–22
- [7] Yaroslavov A A, Sitnikova T A, Rakhnyanskaya A A, Ermakov Y A, Burova T V, Grinberg V Y and Menger F M 2007 *Langmuir* **23** 7539–44
- [8] Sybachin A V, Efimova A A, Litmanovich E A, Menger F M and Yaroslavov A 2007 *Langmuir* **23** 10034–9
- [9] Kamburova K and Radeva T 2007 *J. Colloid Interface Sci.* **313** 398–404
- [10] Pozharski E V and MacDonald R C 2007 *Mol. Pharm.* **4** 962–74
- [11] Bordi F, Cametti C, Sennato S and Truzzolillo D 2007 *Phys. Rev. E* **76** 061403
- [12] Gillies G, Lin W and Borkovec M 2007 *J. Phys. Chem. B* **111** 8626–33
- [13] Sciortino F, Mossa S, Zaccarelli E and Tartaglia P 2004 *Phys. Rev. Lett.* **93** 055701
- [14] Russel W B, Saville D A and Schowalter W R 1989 *Colloidal Dispersions* (Cambridge: Cambridge University Press)
- [15] Mossa S, Sciortino F, Zaccarelli E and Tartaglia P 2004 *Langmuir* **20** 10756–63
- [16] Groenewold J and Kegel W K 2001 *J. Phys. Chem. B* **105** 11702–9
- [17] Campbell A I, Anderson V J, van Duijneveldt J S and Bartlett P 2005 *Phys. Rev. Lett.* **94** 208301
- [18] Sanchez R and Bartlett P 2005 *J. Phys.: Condens. Matter* **17** S3551–6
- [19] Archer A and Wilding N 2007 *Phys. Rev. E* **76** 031501
- [20] Lu P J, Conrad J C, Wyss H M, Schofield A B and Weitz D A 2006 *Phys. Rev. Lett.* **96** 028306
- [21] Bordi F, Cametti C, De Luca F, Gaudino D, Gili T and Sennato S 2003 *Colloids Surf. B* **29** 149–57
- [22] Claessona P, Dedinaitea A and Rojasa O 2003 *Adv. Colloid Interface Sci.* **104** 53–74
- [23] Bremmell K and Scales P 2004 *Colloids Surf. A* **247** 19–25
- [24] Ohshima H 2008 *J. Colloid Interface Sci.* **328** 3–9
- [25] Mou J, Czajkowsky D M, Zhang Y and Shao Z 1995 *FEBS Lett.* **371** 279–82
- [26] Nguyen T T, Grosberg A Y and Shklovskii B I 2000 *Phys. Rev. Lett.* **85** 1568–71
- [27] Dobrynin A V, Deshkovski A and Rubinstein M 2000 *Phys. Rev. Lett.* **84** 3101–4
- [28] Grosberg A Y, Nguyen T T and Shklovskii B I 2002 *Rev. Mod. Phys.* **74** 329–45
- [29] Pericet-Camara R and Papastavrou G B M 2004 *Langmuir* **20** 3264
- [30] Pianegonda S, Barbosa M C and Levin Y 2005 *Europhys. Lett.* **71** 831–7
- [31] Lenz O and Holm C 2008 *Eur. Phys. J. E* **26** 191–5
- [32] Velegol D and Thwar P 2001 *Langmuir* **17** 7687–93
- [33] Sennato S, Bordi F and Cametti C 2004 *Europhys. Lett.* **68** 296–302
- [34] Keren K, Soen Y, Ben Yoseph G, Yechiel R, Braun E, Sivan U and Talmon Y 2002 *Phys. Rev. Lett.* **89** 88103–6
- [35] Kabanov V A, Sergeev V G, Pyshkina O A, Zinchenko A A, Zezin A B, Joosten J G H, Brackman J and Yoshikawa K 2000 *Macromolecules* **33** 9587–93
- [36] Milkova V, Kamburova K, Petkanchin I and Radeva T 2008 *Langmuir* **24** 9495–9
- [37] Radler J O, Koltover I, Jamieson A, Salditt T and Safinya C R 1998 *Langmuir* **14** 4272–83
- [38] Sennato S, Bordi F, Cametti C, Marianecchi C, Carafa M and Cametti M 2008 *J. Phys. Chem. B* **112** 3720–7
- [39] Bordi F, Cametti C, Diociaiuti M and Sennato S 2005 *Phys. Rev. E* **71** 050401
- [40] De Vos C, Deriemaeker L and Finsy R 1996 *Langmuir* **12** 2630–6
- [41] Bordi F, Cametti C, Sennato S and Viscomi D 2007 *J. Chem. Phys.* **126** 024902
- [42] Bordi F, Cametti C, Marianecchi C and Sennato S 2005 *J. Phys.: Condens. Matter* **17** S3423–32
- [43] Yaroslavov A, Kiseliova E, Udalykh O and Kabanov V 1998 *Langmuir* **14** 5160–3
- [44] Gerelli Y, Barbieri S, Di Bari M T, Deriu A, Cantu L, Brocca P, Sonvico F, Colombo P, May R and Motta S 2008 *Langmuir* **24** 11378–84
- [45] Sennato S, Bordi F, Cametti C, Diociaiuti M and Malaspina M 2005 *Biochim. Biophys. Acta* **1714** 11–24
- [46] Ciani L, Ristori S, Salvati A, Calamai L and Martini G 2004 *Biochim. Biophys. Acta* **1664** 70–9
- [47] Zuzzi S, Cametti C and Onori G 2008 *Langmuir* **24** 6044–9
- [48] Israelachvili J N 1985 *Intermolecular and Surface Forces* (London: Academic)
- [49] Harries D, May S, Gelbart W M and Ben-Shaul A 1998 *Biophys. J.* **75** 159–73
- [50] Huebner S, Battersby B and Cevc G 1999 *Biophys. J.* **76** 3158–66
- [51] Safinya C R 2001 *Curr. Opin. Struct. Biol.* **11** 440
- [52] Rodriguez-Pulido A, Ortega F, Llorca O, Aicart E and Junquera E 2008 *J. Phys. Chem. B* **112** 12555–65
- [53] Bordi F, Cametti C, Sennato S and Viscomi D 2006 *J. Colloid Interface Sci.* **304** 512–7
- [54] Logisz C C and Hovis J S 2005 *Biochim. Biophys. Acta* **1717** 104–8
- [55] Yaroslavov A, Kul'kov V E, Polinsky A S, Baibakov B A and Kabanov V 1994 *FEBS Lett.* **340** 121–3
- [56] Kabanov V A and Yaroslavov A 2002 *J. Control. Release* **78** 267–71
- [57] Yaroslavov A, Efimova A A, Lobyshev V and Kabanov V A 2002 *Biochim. Biophys. Acta* **1560** 14–24
- [58] Menger F M, Seredyuk V A, Kitaeva M V, Yaroslavov A A and Melik-Nubarov N S 2003 *J. Am. Chem. Soc.* **125** 2846–7
- [59] Yaroslavov A A, Kuchenkova O, Okuneva I, Melik-Nubarov N S, Kozlova N, Lobyshev V, Menger F M and Kabanov V A 2003 *Biochim. Biophys. Acta* **1611** 44–54
- [60] Hammes G G and Schullery S E 1970 *Biochemistry* **9** 2555–63

- [61] Gad A 1983 *Biochim. Biophys. Acta* **728** 377–82
- [62] Walter A, Steer C J and Blumenthal R 1986 *Biochim. Biophys. Acta* **861** 319–30
- [63] Kozlova N, Bruskovskaya I, Melik-Nubarov N, Yaroslavov A, Kabanov V and Menger F 2001 *Biochim. Biophys. Acta* **1514** 139–51
- [64] Miller I R and Bach D 1974 *Chem. Phys. Lipids* **13** 453–65
- [65] Carrier D and Pézolet M 1984 *Biophys. J.* **46** 497–506
- [66] Bordi F, Cametti C and Paradossi G 1999 *Phys. Chem. Chem. Phys.* **1** 1555–61
- [67] Chittchang M, Alur H, Mitra A and Johnston T P 2002 *J. Pharm. Pharmacol.* **54** 315–23
- [68] Rädler J O, Koltover I, Salditt T and Safinya C R 1997 *Science* **275** 810–4
- [69] Koltover I, Salditt T and Safinya C R 1999 *Biophys. J.* **77** 915–24
- [70] Bruinsma R 1998 *Eur. Phys. J. B* **4** 75–88
- [71] May S, Harries D and Ben-Shaul A 2000 *Biophys. J.* **78** 1681–97
- [72] Dobrynin A V and Rubinstein M 2005 *Prog. Polym. Sci.* **30** 1049–118
- [73] Nylander T, Samoshina Y and Lindman B 2006 *Adv. Colloid Interface Sci.* **123–126** 105–23
- [74] Clausen-Schaumann H and Gaub H E 1999 *Langmuir* **15** 8246–51
- [75] Fang Y and Yang J 1997 *J. Phys. Chem. B* **101** 441–9
- [76] Pitard B, Aguerre O, Airiau M, Lachages A-M, Boukhnikachvili T, Byk G, Dubertret C, Herviou C, Scherman D, Mayaux J-F and Crouzet J 1997 *Proc. Natl Acad. Sci. USA* **94** 14412–7
- [77] Wu C-M, Liou W, Chen H-L, Lin T-L and Jeng U-S 2004 *Macromolecules* **37** 4974–80
- [78] Fleer G, Cohen-Stuart M, Scheutjens J, Cosgrove T and Vincent B 1993 *Polymers at Interfaces* (London: Chapman and Hall)
- [79] Ahrens H, Baltes H, Schmitt J, Möhwald H and Helm C A 2001 *Macromolecules* **34** 4504–12
- [80] Boroudjerdi H, Kim Y-W, Naji A, Netz R R, Schlagberger X and Serr A 2006 *Phys. Rep.* **416** 129–99
- [81] Théodoly O, Ober R and Williams C 2001 *Eur. Phys. J. E* **5** 51–8
- [82] Truzzolillo D, Bordi F, Cametti C and Sennato S 2008 *Colloids Surf. A* **319** 51–61
- [83] Netz R R and Joanny J-F 1999 *Macromolecules* **32** 9013–25
- [84] Netz R R and Joanny J-F 1999 *Macromolecules* **32** 9026–40
- [85] Netz R R and Andelman D 2003 *Phys. Rep.* **380** 1–95
- [86] Manning G S 1969 *J. Chem. Phys.* **51** 924–33
- [87] Oosawa F 1971 *Polyelectrolytes* (New York: Dekker)
- [88] Manning G S 1978 *Q. Rev. Biophys.* **11** 179–246
- [89] Bordi F, Cametti C and Colby R H 2004 *J. Phys.: Condens. Matter* **16** R1423–63
- [90] Borukhov I, Andelman D and Orland H 1998 *Macromolecules* **31** 1665–71
- [91] de Meijere K, Brezesinski G and Möhwald H 1997 *Macromolecules* **30** 2337–42
- [92] de Gennes P G 1980 *Scaling Concepts in Polymer Physics* (Ithaca, NY: Cornell University Press)
- [93] Grosberg A Y and Khokhlov A R 1994 *Statistical Physics of Macromolecules* (New York: AIP Press)
- [94] Dobrynin A, Colby R H and Rubinstein M 1995 *Macromolecules* **28** 1859
- [95] Dobrynin A V, Deshkovski A and Rubinstein M 2001 *Macromolecules* **34** 3421–36
- [96] Nguyen T T and Shklovskii B I 1999 *Phys. Rev. Lett.* **82** 3268–71
- [97] Netz R and Andelman D 2002 Polyelectrolytes in solution and at surfaces *Encyclopedia of Electrochemistry* vol 1, ed M Urbakh and E Giladi (Weinheim: Wiley-VCH) (arXiv:cond-mat/0101314 v2)
- [98] Schmitz K S and Yu J-W 1988 *Macromolecules* **21** 484–93
- [99] Vagharchakian L and Hénon S 2003 *Langmuir* **19** 7989–94
- [100] Truzzolillo D, Bordi F, Cametti C and Sennato S 2009 *Phys. Rev. E* **79** 011804
- [101] Odijk J 1977 *J. Polym. Sci.* **15** 477–83
- [102] Nguyen T T and Shklovskii B I 2001 *Phys. Rev. E* **64** 041407
- [103] Nguyen T T and Shklovskii B I 2002 *Phys. Rev. Lett.* **89** 018101
- [104] Nguyen T T and Shklovskii B I 2002 *Physica A* **310** 197–211
- [105] Walker W H and Grant S B 1996 *Colloids Surf. A* **119** 229–39
- [106] Larsen A E and Grier D G 1997 *Nature* **385** 230–3
- [107] Leong Y K 2001 *Colloid Polym. Sci.* **279** 82–7
- [108] Butler J, Angelini T, Tang J and Wong G 2003 *Phys. Rev. Lett.* **91** 028301
- [109] Wong G C L, Lin A, Tang J X, Li Y, Janmey P A and Safinya C R 2003 *Phys. Rev. Lett.* **91** 018103
- [110] Granfeldt M K, Joansson B and Woodward C E 1991 *J. Phys. Chem.* **95** 4819–26
- [111] Grønbech-Jensen N, Mashl R J, Bruinsma R F and Gelbart W M 1997 *Phys. Rev. Lett.* **78** 2477–80
- [112] Wu J, Bratko D and Prausnitz J M 1998 *Proc. Natl Acad. Sci. USA* **95** 15169–72
- [113] Linse P and Lobaskin V 1999 *Phys. Rev. Lett.* **83** 4208
- [114] Linse P 2002 *J. Phys.: Condens. Matter* **14** 13449–67
- [115] Messina R, Holm C and Kremer K 2000 *Phys. Rev. Lett.* **85** 872
- [116] Messina R, Holm C and Kremer K 2002 *Comput. Phys. Commun.* **147** 282
- [117] Dzubiella J, Moreira A G and Pincus P A 2003 *Macromolecules* **36** 1741–52
- [118] Najia A and Netz R 2004 *Eur. Phys. J. E* **13** 43–59
- [119] Lau A W C and Pincus P 1998 *Phys. Rev. Lett.* **81** 1338–41
- [120] Olvera de la Cruz M, Belloni L, Delsanti M, Dalbiez J P, Spalla O and Drifford M 1995 *J. Chem. Phys.* **103** 5781–91
- [121] Rouzina I and Bloomfield V A 1996 *J. Phys. Chem.* **100** 9977
- [122] Miklavic S J, Chan D Y C, White L R and Healy T W 1994 *J. Phys. Chem.* **98** 9022–32
- [123] Khachatourian A V M and Wistrom A O 1998 *J. Phys. Chem. B* **102** 2483–93
- [124] Totsuji H 1978 *Phys. Rev. A* **17** 399
- [125] Leong Y K, Scales P J, Healy T W and Boger D V 1995 *Colloids Surf. A* **95** 43–52
- [126] Record M, Anderson C F and Lohman T M 1978 *Q. Rev. Biophys.* **11** 103–78
- [127] Park S Y, Bruinsma R F and Gelbart W M 1999 *Europhys. Lett.* **46** 454–60
- [128] Wagner K, Harries D, May S, Kahl V, Rädler J O and Ben-Shaul A 2000 *Langmuir* **16** 303–6
- [129] Simberg D, Danino D, Talmon Y, Minsky A, Ferrari M E, Wheeler C J and Barenholz Y 2001 *J. Biol. Chem.* **276** 47453–9
- [130] Alexander S, Chaikin P, Grant P, Morales G J, Pincus P and Hone D 1984 *J. Chem. Phys.* **80** 5776–81
- [131] Bordi F, Cametti C, Sennato S, Paoli B and Marianecchi C 2006 *J. Phys. Chem. B* **110** 4808–14
- [132] Belloni L 1998 *Colloids Surf. B* **140** 227
- [133] Taheri-Araghi S and Ha B-Y 2005 *Phys. Rev. E* **72** 021508
- [134] Haro-Pérez C, Quesada-Pérez M, Callejas-Fernández J, Casals E, Estelrich J and Hidalgo-Álvarez R 2003 *J. Chem. Phys.* **118** 5167–73
- [135] Wette P, Schöpe H J and Palberg T 2002 *J. Chem. Phys.* **24** 10981–8
- [136] Quesada-Pérez M, Callejas-Fernández J and Hidalgo-Álvarez A R 2002 *Adv. Colloid Interface Sci.* **95** 295–315
- [137] Mukherjee A K, Schmitz K S and Bhuiyan L B 2002 *Langmuir* **18** 4210–9
- [138] Sanghiran V and Schmitz K S 2000 *Langmuir* **16** 7566–74
- [139] Spink C H and Chaires J B 1997 *J. Am. Chem. Soc.* **119** 10920–8

- [140] Kennedy M, Pozharski E, Rakhmanova V and Mac Donald R 2000 *Biophys. J.* **78** 1620–33
- [141] Pozharski E and MacDonald R C 2002 *Biophys. J.* **83** 556–65
- [142] Gonçalves E, Debs R J and Heath T D 2004 *Biophys. J.* **86** 1554–63
- [143] Lobo B A, Davis A, Koe G, Smith J G and Middaugh C R 2001 *Arch. Biochem. Biophys.* **386** 95–105
- [144] Fleck C and von Grünberg H H 2001 *Phys. Rev. E* **63** 061804
- [145] Sens P and Joanny J-F 2000 *Phys. Rev. Lett.* **84** 4862–5
- [146] Grosse C 2002 Relaxation mechanisms of homogeneous particles and cells suspended in aqueous electrolyte solutions *Interfacial Electrokinetics and Electrophoresis* vol 106, ed A V Delgado (New York: Dekker) pp 277–327
- [147] Kallay N 1999 *Interfacial Dynamics (Surfactant Science)* (New York: Dekker)
- [148] Feldman Y, Skodvin T and Sjöblom J 2001 Dielectric spectroscopy on emulsion and related colloidal systems. A review *Encyclopedic Handbook of Emulsion Technology* ed J Sjöblom (New York: Dekker) pp 109–68
- [149] Radeva T and Kamburova K 2006 *J. Colloid Interface Sci.* **293** 290–5
- [150] Milkova V and Radeva T 2006 *J. Colloid Interface Sci.* **298** 550–5
- [151] Shin Y, Roberts J E and Santore M M 2002 *J. Colloid Interface Sci.* **247** 220–30
- [152] Bordi F, Cametti C, Sennato S and Viscomi D 2006 *Phys. Rev. E* **74** 030402(R)
- [153] Nguyen T T and Shklovskii B I 2001 *J. Chem. Phys.* **114** 5905–16
- [154] Nguyen T T and Shklovskii B I 2001 *J. Chem. Phys.* **115** 7298–308
- [155] Nguyen T T and Shklovskii B I 2001 *Physica A* **293** 324–38
- [156] Truzzolillo D, Bordi F, Sciortino F and Cametti C 2008 arXiv:cond-mat.soft 0804 0781v2
- [157] Sennato S, Truzzolillo D, Bordi F and Cametti C 2008 *Langmuir* **24** 12181–8
- [158] Hogg R, Healy T W and Fuerstenau D W 1966 *Trans. Faraday Soc.* **62** 1638
- [159] Todd B and Eppell S J 2004 *Langmuir* **20** 4892–7
- [160] Nguyen T T and Shklovskii B I 2002 *Phys. Rev. E* **65** 031409
- [161] Griffin G L and Andres R P 1979 *J. Chem. Phys.* **71** 2522–30
- [162] Tadmor R 2001 *J. Phys.: Condens. Matter* **13** L195–202
- [163] Israelachvili J N 1994 *Langmuir* **10** 3369–70
- [164] Petsev D N 1999 *Langmuir* **15** 1096–100
- [165] Sabín J, Prieto G, Messina P, Ruso J M, Hidalgo-Alvarez R and Sarmiento F 2005 *Langmuir* **21** 10968–75
- [166] Petrache H I, Zemb T, Belloni L and Parsegian V A 2006 *Proc. Natl Acad. Sci.* **103** 7982–7
- [167] Warren P 2000 *J. Chem. Phys.* **112** 4683–98
- [168] Sciortino F, Buldyrev S V, De Michele C, Foffi G, Ghofraniha N, La Nave E, Moreno A, Mossa S, Saika-Voivod I, Tartaglia P and Zaccarelli E 2005 *Comput. Phys. Commun.* **169** 166–71
- [169] Zaccarelli E 2007 *J. Phys.: Condens. Matter* **19** 323101
- [170] Rayburn E, Wang H, He J and Zhang R 2005 *Lett. Drug Design Discov.* **2** 1–18
- [171] Siomi H and Siomi M C 2009 *Nature* **457** 396–404  
Jinek M and Doudna J A 2009 *Nature* **457** 405–12  
Castanotto D and Rossi J J 2009 *Nature* **457** 426–33
- [172] Mouritsen O G 2005 *Life—as a Matter of Fat* (Berlin: Springer)
- [173] El-Anead A 2004 *J. Control. Release* **94** 1–14
- [174] Zhang S, Xu Y, Wang B, Qiao W, Liu D and Li Z 2004 *J. Control. Release* **100** 165–80
- [175] Wasungu L and Hoekstra D 2006 *J. Control. Release* **116** 255–64
- [176] Lichterfeld M, Qurishi N, Hoffmann C, Hochdorfer B, Brockmeyer N H, Arasteh K, Mauss S and Rockstroh J K 2004 *Infection* **33** 140–7
- [177] Lanao J, Briones E and Colino C I 2007 *J. Drug Target.* **15** 21–36
- [178] Pierson T, McArthur J and Siliciano R F 2000 *Annu. Rev. Immunol.* **18** 665–708
- [179] Walker B and Burton D R 2008 *Science* **320** 760–4
- [180] Huwyler J J D and Krähenbühl S 2008 *Int. J. Nanomed.* **3** 21–9
- [181] Fraenkel-Conrat H and Williams R C 1955 *Proc. Natl Acad. Sci. USA* **41** 690–8
- [182] Van Workum K and Douglas J F 2006 *Phys. Rev. E* **73** 031502
- [183] Muthukumar M, Ober C and Thomas E 1997 *Science* **277** 1225–32
- [184] Stupp S and Braun P 1997 *Science* **277** 1242–8
- [185] Lasic D 1997 *Liposomes in Gene Delivery* (Boca Raton, FL: CRC Press)
- [186] Lasic D 1998 *Trends Biotechnol.* **16** 307–21
- [187] Khalil I, Kogure K, Futaki S and Harashima H 2008 *Int. J. Pharm.* **354** 39–48
- [188] Li J and Loh X J 2008 *Adv. Drug Deliv. Rev.* **60** 1000–17